

Lecture Notes Black Holes and Gravitational Waves

Maarten van de Meent

April 2024

Contents

1	Penrose Diagrams	3
1.1	Conformal transformations	3
1.2	Minkowski space	3
1.3	Schwarzschild	6
1.3.1	Definition of a Black Hole	8
1.3.2	Spherical collapse	9
1.4	The Kerr Black Hole	10
1.4.1	Collapse of a rotating black hole	12
2	Geodesics in Kerr Spacetime	15
2.1	The geodesic equation	15
2.2	Symmetries and Killing vectors	15
2.3	Constants of Motion of Kerr geodesics	18
2.4	Separating the geodesic equations	20
2.5	The polar equation	21
2.6	The radial equation	23
2.6.1	Circular orbits	26
2.7	Characterizing bound orbits	27
2.8	Null geodesics and black hole shadows	29
3	Black Hole Perturbation Theory	31
3.1	Perturbation theory in GR	31
3.2	Linearized Einstein Equation	33
3.3	The Penrose Wave Equation	35
3.4	The Weyl scalars	38
3.5	Teukolsky Equation	39
3.5.1	Separation of Variables	40
3.5.2	Homogeneous solutions, Asymptotic Behaviour, and Boundary conditions	42
3.5.3	Particular solutions	45
3.6	Quasinormal Modes	45

Conventions

We will be using the following conventions through out these notes.

- We work in geometric units such that $G = c = 1$.
- We utilize **abstract index notation** to refer to tensors. This means that abstract tensors are always denoted with indices that indicate the type and rank of the tensor. This does not signify that any particular coordinate basis has been chosen. Repeated indices of opposite type will denote contractions.
- Parentheses $()$ around a set of indices indicated the symmetrization of those indices, e.g.

$$T_{(\mu_1 \cdots \mu_n)} = \frac{1}{n!} \sum_{\sigma \in S_n} T_{\mu_{\sigma(1)} \cdots \mu_{\sigma(n)}},$$

where S_n is the group of all permutations of n characters.

- Square brackets $[]$ around a set of indices indicated the anti-symmetrization of those indices, e.g.

$$T_{[\mu_1 \cdots \mu_n]} = \frac{1}{n!} \sum_{\sigma \in S_n} \text{sign}(\sigma) T_{\mu_{\sigma(1)} \cdots \mu_{\sigma(n)}},$$

where $\text{sign}(\sigma)$ is the parity of the permutation σ .

Chapter 1

Penrose Diagrams

Literature:

- Reall, Chap. 5
- Carroll, Sec. 5.6, 5.7 and Appendix H

In this chapter we will develop the tools to describe the causal structure of a spacetime, allowing us to define what it means for a spacetime to contain a black hole.

1.1 Conformal transformations

Given a metric $g_{\mu\nu}$ on a spacetime M , we can define a new metric $\bar{g}_{\mu\nu}$ as $\bar{g}_{\mu\nu} = \omega(x)^2 g_{\mu\nu}$, where $\omega : M \rightarrow \mathbb{R}$ is a positive smooth function. This new metric $\bar{g}_{\mu\nu}$ in general defines a new spacetime geometry. Nonetheless, this new geometry will agree with the old geometry on the notions of curves being “timelike”, “spacelike”, or “null”, i.e. they will agree on the possible causal relations between different spacetime events; the **causal structure** of the spacetime. The transformation from $g_{\mu\nu}$ to $\bar{g}_{\mu\nu}$ encoded by the function $\omega(x)$ is known as a **conformal transformation**, since it preserves the angles (but not lengths) of the geometry.

The idea is to use these conformal transformations to take a (generally infinite) spacetime and map it to a compact spacetime (which we can draw on a page) with the same causal structure.

1.2 Minkowski space

We start with the Minkowski space. In spherical coordinates the Minkowski metric reads

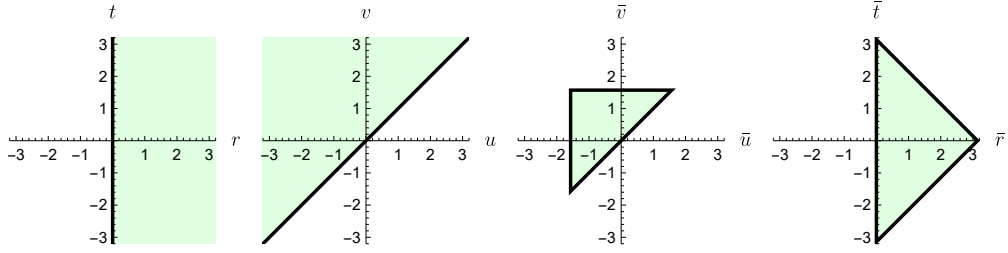


Figure 1.1: Illustration of the ranges of the different coordinates used in this section.

$$\eta_{\mu\nu} = -dt^2 + dr^2 + r^2(d\theta^2 + \sin^2\theta d\phi^2), \quad (1.1)$$

with the coordinate ranges (which will become important later on) $t \in (-\infty, \infty)$, $r \in [0, \infty)$, $\theta \in [0, \pi]$, and $\phi \in [-\pi, \pi]$. Our first step is to define lightcone coordinates

$$u = t - r, \quad \text{and} \quad v = t + r, \quad (1.2)$$

which gives the metric

$$\eta_{\mu\nu} = -dudv + \frac{1}{4}(v - u)^2(d\theta^2 + \sin^2\theta d\phi^2), \quad (1.3)$$

with ranges $-\infty < u \leq v < \infty$. We can compactify the range of our coordinates by choosing new coordinates (\bar{u}, \bar{v}) defined by,

$$u = \tan \bar{u}, \quad \text{and} \quad v = \tan \bar{v}, \quad (1.4)$$

which reduces the ranges to $-\pi/2 < \bar{u} \leq \bar{v} < \pi/2$, and gives the metric

$$\eta_{\mu\nu} = (2 \cos \bar{u} \cos \bar{v})^{-2} (-4d\bar{u}d\bar{v} + \sin^2(\bar{v} - \bar{u})(d\theta^2 + \sin^2\theta d\phi^2)). \quad (1.5)$$

To find the conformal compactification of Minkowski space, we finally define the function

$$\omega = 2 \cos \bar{u} \cos \bar{v}, \quad (1.6)$$

and the coordinates

$$\bar{t} = \bar{u} + \bar{v}, \quad \text{and} \quad \bar{r} = \bar{v} - \bar{u}, \quad (1.7)$$

to find the metric

$$\bar{\eta}_{\mu\nu} = -d\bar{t}^2 + d\bar{r}^2 + \sin^2 \bar{r}(d\theta^2 + \sin^2\theta d\phi^2). \quad (1.8)$$

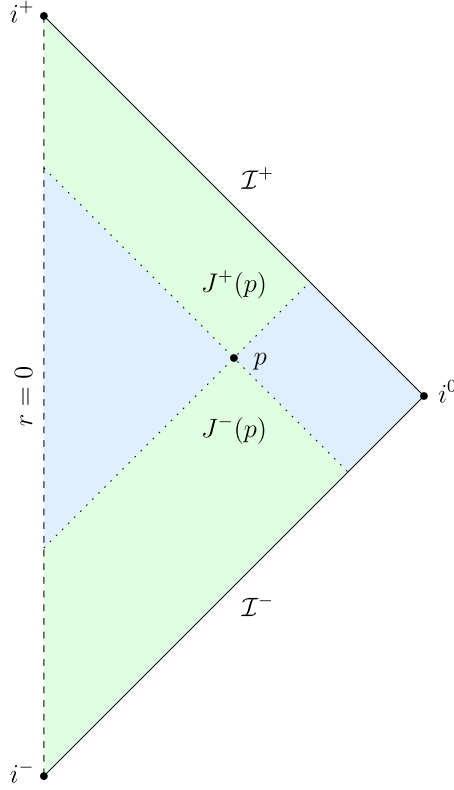


Figure 1.2: The Penrose diagram for Minkowski space.

The astute reader may recognize this as the line element of the Einstein static universe, $\mathbb{R} \times S^3$ (see Harmark Ex. 4.3). However, the crucial difference lies in the range of the coordinates, in particular $0 \leq \bar{r} < \pi$ and $-\pi + \bar{r} < \bar{t} < \pi - \bar{r}$ (see Fig. 1.1). By projecting onto the (\bar{r}, \bar{t}) -plane, we obtain the **Penrose diagram** for Minkowski space, shown in Fig. 1.2. Each interior point of the shown region represents a 2-sphere in the full spacetime. The dashed boundary at $\bar{r} = 0$ represents the symmetry axis at $r = 0$ of the original coordinates, and the outer boundary denotes the points originally “at infinity”.

To understand the structure of “infinity” we can consider the behavior of radial geodesics in the diagram. By construction of the diagram all radial null geodesics travel along 45 degree lines. Any null geodesic will originate at \mathcal{I}^- , travel along an inwards 45 degree straight line until it reaches $r = 0$, and reflect back to an outwards 45 degree line until it reaches \mathcal{I}^+ . We therefore refer to \mathcal{I}^- as **past null infinity**, and \mathcal{I}^+ as **future null infinity**. In a similar vein, all radial spacelike geodesics start and end at i^0 , which we call

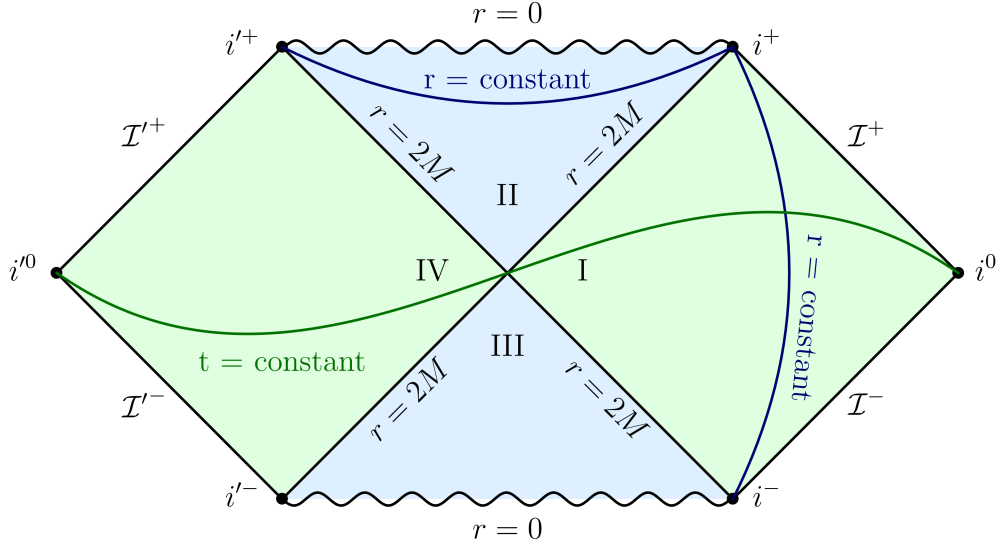


Figure 1.3: The Penrose diagram for the maximally extended Schwarzschild spacetime.

spatial infinity, and timelike geodesics start at i^- and end at i^+ , which are called **past** and **future timelike infinity**, respectively.

A spacetime whose Penrose diagram has a structure near infinity resembling¹ that of Minkowski space is called **asymptotically flat**.

Finally, we use the Penrose diagram of Minkowski space to visualize to more important concepts related to the causal structure of spacetime. Given an event $p \in M$, the set of all events that can be connected to p with a future-directed causal (i.e. timelike or null) curve ending in p , is called the **causal past of p** , and denoted $J^-(p)$. In the Penrose diagram the intersection of $J^-(p)$ with a constant (θ, ϕ) -slice is simply the 45-degree wedge below the point p as shown in Fig. 1.2. Similarly, the set of all events that can be connected to p with a future-directed causal (i.e. timelike or null) curve starting at p , is called the **causal future of p** , and denoted $J^+(p)$.

1.3 Schwarzschild

In the course by Harmark you were introduced to the Schwarzschild metric,

¹For a more precise technical discussion of what “resembling” means in this context, see Chapter 5 of Reall’s lecture notes.

$$g_{\mu\nu} = -\left(1 - \frac{2M}{r}\right)dt^2 + \frac{dr^2}{1 - \frac{2M}{r}} + r^2(d\theta^2 + \sin^2\theta d\phi^2). \quad (1.9)$$

This metric has a (coordinate) singularity at $r = 2M$. Consequently, the a priori domain of the coordinates is $-\infty < t < \infty$ and $2M < r < \infty$. By changing the time coordinate to (advanced) Eddington-Finkelstein time

$$v = t + r^* \quad \text{with} \quad r^* = r + 2M \log\left(\frac{r - 2M}{2M}\right), \quad (1.10)$$

you were shown that the validity of the Schwarzschild metric can be extended to $0 < r < \infty$ for infalling observers. The same reasoning can be applied when using the retarded Eddington-Finkelstein time coordinate $u = t - r^*$ to show that there exists an (inequivalent) extension of Schwarzschild to the past of outgoing observers. When using both u and v to form double null coordinates we obtain

$$g_{\mu\nu} = -\left(1 - \frac{2M}{r(u,v)}\right) du dv + r(u,v)^2(d\theta^2 + \sin^2\theta d\phi^2). \quad (1.11)$$

Even with the maximal coordinate range $-\infty < u, v < \infty$ these coordinates correspond only to the $2M < r < \infty$ Schwarzschild patch. The $r = 2M$ boundary corresponds to the $u \rightarrow \infty$ and $v \rightarrow -\infty$ limits. To find coordinates that cover all of the extended spacetime we introduce rescaled null coordinates

$$u = -4M \log(-\underline{u}) \quad \text{and} \quad v = 4M \log(\underline{v}). \quad (1.12)$$

In these coordinates the original Schwarzschild patch is covered by $-\infty < \underline{u} < 0$ and $0 < \underline{v} < \infty$. With these coordinates the Schwarzschild metric takes its **Kruskal-Szekeres** form,

$$g_{\mu\nu} = -\frac{32M}{r(\underline{u}, \underline{v})} e^{-\frac{r}{2M}} d\underline{u} d\underline{v} + r(\underline{u}, \underline{v})^2(d\theta^2 + \sin^2\theta d\phi^2), \quad (1.13)$$

where r is defined implicitly through the relation $\underline{u} \underline{v} = (r/(2M) - 1)e^{r/(2M)}$. This form is manifestly smooth at $\underline{u} = 0$ and $\underline{v} = 0$ (i.e. $r = 2M$), and be extended beyond this point.

To produce the Penrose diagram we can again compactify the range of \underline{u} and \underline{v} by introducing

$$\underline{u} = \tan \bar{u}, \quad \text{and} \quad \underline{v} = \tan \bar{v}, \quad (1.14)$$

and an appropriate conformal factor ω such that we obtain a compactified metric of the form

$$\bar{g}_{\mu\nu} = -2d\bar{u}d\bar{v} + R(\bar{u}, \bar{v})^2(d\theta^2 + \sin^2\theta d\phi^2). \quad (1.15)$$

(the explicit form of ω and R is messy and not particularly illuminating).

The resulting Penrose diagram is shown in Fig. 1.3. The original Schwarzschild patch (marked “I”) is asymptotically flat. The original (advanced) Eddington-Finkelstein coordinates extend the metric to region “II” allowing objects to fall into the black hole and reach the singularity at $r = 0$. The corresponding construction with the retarded time extends the metric to region “III”, allowing the worldline to extend to the singularity in their past.

Finally, we are presented with a second asymptotically flat region (“IV”), complete with its own copies of future and past null infinity (\mathcal{I}^+ and \mathcal{I}^-), future and past timelike infinity (i'^+ and i'^-), and spacelike infinity i'^0 . There are no causal curves that connect regions I and IV. So, for an observer in region I, region IV might as well not exist, and vice versa. There are however spacelike curves that connect regions I and IV. This “worm hole” between “parallel universes” is known as an **Einstein-Rosen bridge**. Because it consists solely of spacelike curves, there is no way to transverse it.

1.3.1 Definition of a Black Hole

We are now ready to give a precise definition of a black hole:

Definition 1. Let $(M, g_{\mu\nu})$ be a spacetime that is asymptotically flat at null infinity. The **black hole region** is $\mathcal{B} = M \setminus J^-(\mathcal{I}^+)$. The boundary of \mathcal{B} , $\partial\mathcal{B}$ is called the **future event horizon**, \mathcal{H}^+ . Similarly, $\mathcal{W} = M \setminus J^+(\mathcal{I}^-)$ is the **white hole region**, and its boundary $\partial\mathcal{W}$, the **past event horizon**, \mathcal{H}^- .

In more plain English a black hole consists of those events in spacetime from which no signal can reach future null infinity, a white hole consists of those events which cannot be reached by any signal starting at past null infinity. A direct consequence of this definition is that an event horizon is always a null-surface.

Concretely, when we look at the Penrose diagram for Schwarzschild in Fig. 1.3, we see that the black hole region \mathcal{B} corresponding to \mathcal{I}^+ consists of the union of regions II and IV, and the future event horizon \mathcal{H}^+ is the boundary $\bar{u} = 0$, where $r = 2M$. The white hole region \mathcal{W} is the union of regions III and IV, and the past event horizon is \mathcal{H}^- is the boundary $\bar{v} = 0$, where $r = 2M$ as well.

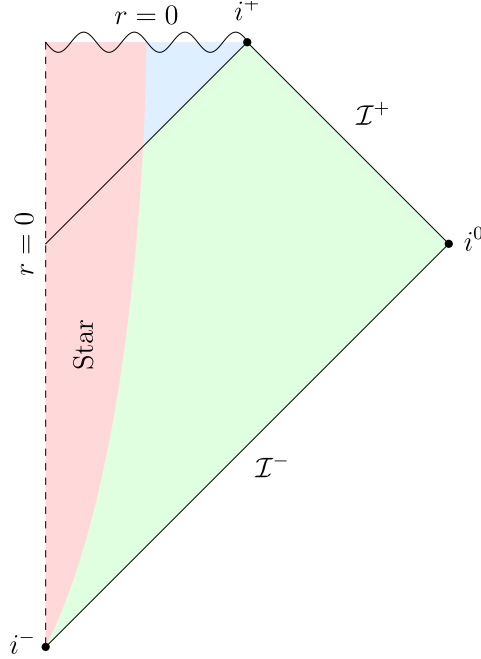


Figure 1.4: The Penrose diagram for a spherically symmetric star collapsing to a black hole.

Note that since the maximally extended Schwarzschild spacetime has two asymptotically flat regions, each region has its own black (white) hole regions. Relative to \mathcal{I}^+ the black hole consists of the unions of I and II, and relative to \mathcal{I}^- the white hole consists of regions I and III.

1.3.2 Spherical collapse

The maximally extended Schwarzschild solution contains some fantastical features (wormholes, parallel universes, etc.). A good question to ask ourselves is which of these features arise from the strict symmetry constraints (vacuum, spherical symmetry, static), and which features survive in a more realistic scenario. To this end we display the Penrose diagram for a spherically symmetric star collapsing to a black hole in Fig. 1.4. Outside of the star, the spacetime is spherically symmetric and vacuum, and therefore — by Birkhoff's theorem — given by the Schwarzschild solution. The interior of the star, which encapsulates $r = 0$ at early times, is given by a more regular solution.

We see that the only fantastical feature that remain is the formation of an event horizon, black hole region, and singularity. All the more science

fiction sounding features like white holes, worm holes, and parallel universes have disappeared due to the inclusion of a matter distribution.

1.4 The Kerr Black Hole

The Kerr solution for a rotating black hole was introduced in Sec. 3.3 of Harmark's notes. In Boyer-Lindquist coordinates it is given by

$$g_{\mu\nu} = - \left(1 - \frac{2Mr}{\Sigma} \right) dt^2 - \frac{4Mar}{\Sigma} \sin^2 \theta dt d\phi \\ + \frac{(r^2 + a^2)^2 - a^2 \Delta \sin^2 \theta}{\Sigma} \sin^2 \theta d\phi^2 + \frac{\Sigma}{\Delta} dr^2 + \Sigma d\theta^2, \quad (1.16)$$

with

$$\Sigma(r, \theta) = r^2 + a^2 \cos^2 \theta, \quad \text{and} \quad (1.17)$$

$$\Delta(r) = r^2 - 2Mr + a^2 = (r - r_+)(r - r_-). \quad (1.18)$$

This metric has a trivial coordinate singularity at $\theta = 0$ and $\theta = \pi$, coordinate singularities at $r = r_{\pm} = M \pm \sqrt{M^2 - a^2}$ corresponding to horizons, and a true curvature ring singularity at $r = 0$ and $\theta = \pi/2$.

The coordinate singularities at $r = r_{\pm}$ divide the metric in three disjoint patches ($r_+ < r < \infty$, $r_- < r < r_+$, and $-\infty < r < r_-$) that, a priori, are unrelated. The different patches can be related to each other using a similar procedure as in Schwarzschild using advanced and retarded time coordinates. We will not discuss the details here², instead we simply present the resulting Penrose diagram in Fig. 1.5.

From region I we can again traverse into a black hole by crossing $r = r_+$ into region II. In region II the r direction is timelike and we can only proceed to smaller values of r until we cross $r = r_-$ into region V (or V'). In region the r -direction is again spacelike and worldlines can both proceed to smaller r or (as will be the case for almost all geodesics) back outward to larger r until we cross $r = r_-$ again and enter region III'. Here r is again timelike and we can only proceed further outward until we cross $r = r_+$ into region I', a new distinct copy of region I (or its parallel universe region IV'). From here we can continue ad infinitum to find an infinity stack of new asymptotically flat regions.

In region V we could have also proceeded to $r = 0$. Only for $\theta = \pi/2$ is this a singularity. For all other values of θ we are free to cross into the $r < 0$

²For the full details see [2]

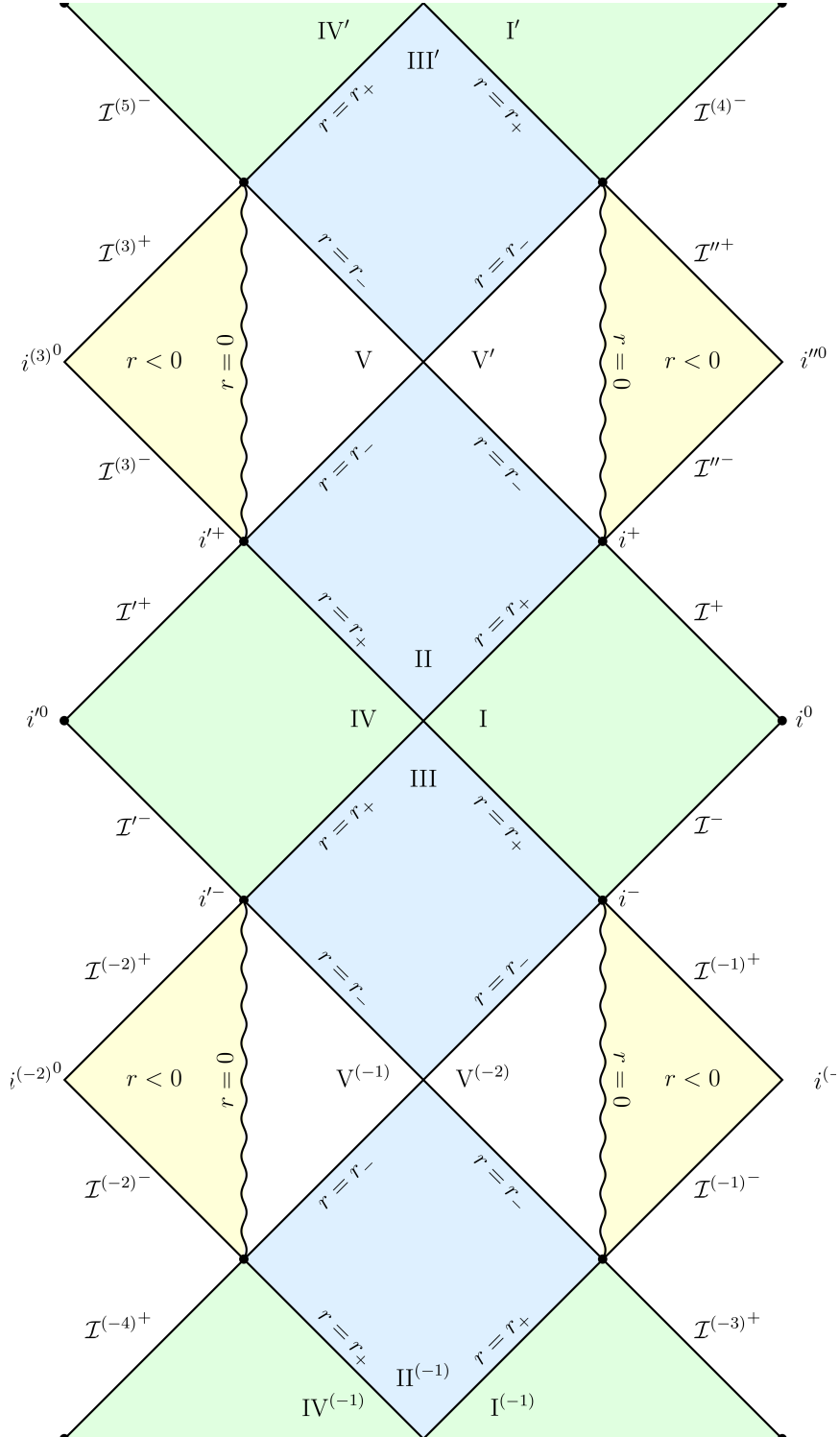


Figure 1.5: The Penrose diagram for a maximally extended Kerr black hole.

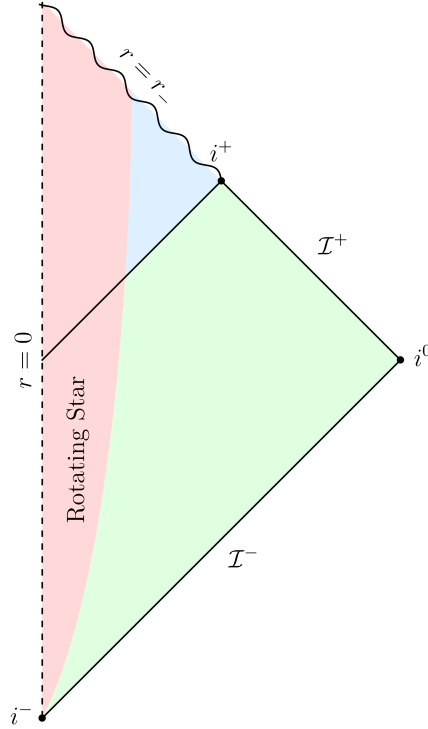


Figure 1.6: A sketch of the Penrose diagram for a rotating star collapsing to a Kerr black hole.

region. This region is again asymptotically flat but now in the $r \rightarrow -\infty$ limit. However, in this region there is no horizon to shield future null infinity from the singularity at $r = 0$, the singularity is **naked**. To make matters worse, this region also has closed timelike curves, breaking causality.

1.4.1 Collapse of a rotating black hole

Maximally extended Kerr is even more fantastical than its non-rotating counterpart. It is therefore a good idea to regain our grounding and look at a more realistic collapse scenario. Unfortunately, there is no equivalent of Birkhoff's theorem for rotating geometries. Consequently, we are not guaranteed that the spacetime outside of the star is exactly Kerr. Instead we have to make do with the much weaker result from the no hair theorem that after the collapse the region outside the horizon has to settle down to a member of the Kerr(-Newman) family.

Most of the really fantastical features of maximally extended Kerr man-

ifest themselves after crossing the $r = r_-$ boundary. How much should we really trust the solution after this point. The first thing to note is that this boundary is a **Cauchy horizon**, meaning that if we try to construct the solution for initial data on some timelike slice this is the absolute limit we can evolve or solutions before singularities start to appear somewhere in our domain of dependence. We should be very wary of the analytically extended version of the solution beyond this point, because it cannot be obtained through a natural evolution. Second, we note that if we take an event on the Cauchy horizon between region II and V' its causal history $J^-(p)$ will actual contain all of region I (for some value of θ). An observer crossing this line is therefore confronted with an infinity amount of history in a finite amount of time. Consequently, even the tiniest perturbation of the spacetime is likely to be blue shifted to something singular. It is therefore conjectured that this Cauchy surface will become singular for generic perturbations away from Kerr.

Based on these conjectures we sketch what the Penrose diagram for a rotating collapsing star likely looks like in Fig. 1.6. The final result looks remarkably like the Schwarzschild case, avoiding the most fantastical behaviour of the maximally extended Kerr.

Chapter 2

Geodesics in Kerr Spacetime

2.1 The geodesic equation

Literature: Harmark, Sec. 1.3.3 and 1.4.6; Carroll Sec. 3.3 and 3.4

In the first GR course you saw the geodesic equation

$$\frac{D}{ds} \frac{dx^\mu}{ds} = \frac{dx^\alpha}{ds} \nabla_\alpha \frac{dx^\mu}{ds} = \frac{d^2 x^\mu}{ds^2} + \Gamma_{\alpha\beta}^\mu \frac{dx^\alpha}{ds} \frac{dx^\beta}{ds} = 0. \quad (2.1)$$

Solving this equation can be made easier by first identifying constants of motion, the existence of which is intertwined with the notion of spacetime symmetries.

2.2 Symmetries and Killing vectors

Literature: Carroll Sec. 3.8 and Appendix B, Wald Appendix C

A symmetry of a spacetime M is a automorphism $\phi : M \rightarrow M$ that leaves the spacetime “invariant”. Infinitesimal automorphisms are given by vector fields in the following way. Suppose we have a (smooth) vector field V^μ , we can construct a family of automorphisms $\phi_{V^\mu}^t$ indexed by a variable $t \in \mathbb{R}$ by mapping each event $p \in M$ to a new event p' by following the integral curves of V^μ for a time t . (I.e. we solve the differential equation $\frac{dx^\mu}{dt} = V^\mu$ with initial condition $x(0) = p$, and set $p' = x(t)$.)

We can try to ask ourselves the question how does a $T_{\mu_1 \dots \mu_n}$ change along the integral lines of V^μ . Naively one may try to write the down the derivative

$$\lim_{t \rightarrow 0} \frac{T_{\mu_1 \dots \mu_n}(p') - T_{\mu_1 \dots \mu_n}(p)}{t}.$$

However, such an expression does not make any mathematical sense. The tensors $T_{\mu_1 \dots \mu_n}(p')$ and $T_{\mu_1 \dots \mu_n}(p)$ belong to (the tensor product of) the

(co)tangent space at different points in M . Consequently, we cannot add (or subtract) them. To get another object that lives at p , we can consider the map induced by $\phi_{V^\mu}^t$ on the tensor bundles (the push forward), or more specifically its inverse (the pull back) $(\phi_{V^\nu}^t)^*$, which in terms of components is given by

$$((\phi_{V^\nu}^t)^* T)_{\mu_1 \dots \mu_n}(p) = \frac{\partial p'^{\alpha_1}}{\partial p^{\mu_1}} \cdots \frac{\partial p'^{\alpha_n}}{\partial p^{\mu_n}} T_{\alpha_1 \dots \alpha_n}(p').$$

This allows us to define a derivative that is defined covariantly and expresses how much a tensor field changes in the direction of a vector field V^μ .

Definition 2. Given a vector field V^μ and a tensor field $T_{\mu_1 \dots \mu_n}$ we can define the **Lie¹ derivative** of $T_{\mu_1 \dots \mu_n}$ w.r.t. V^μ at an event p as follows,

$$\mathcal{L}_{V^\nu} T_{\mu_1 \dots \mu_n}(p) = \lim_{t \rightarrow 0} \frac{((\phi_{V^\nu}^t)^* T_{\mu_1 \dots \mu_n})(p) - T_{\mu_1 \dots \mu_n}(p)}{t}$$

Note that this notion of derivative does not require the existence of a metric. This makes it suitable to explore the symmetries of the metric itself. In particular, if we calculate the Lie derivative of a metric tensor $g_{\mu\nu}$ we find

$$\begin{aligned} \mathcal{L}_{K^\lambda} g_{\mu\nu} &= \lim_{t \rightarrow 0} \frac{((\phi_{V^\nu}^t)^* g_{\mu\nu})(p) - g_{\mu\nu}(p)}{t} \\ &= \lim_{t \rightarrow 0} \frac{\frac{\partial p'^\alpha}{\partial p^\mu} \frac{\partial p'^\beta}{\partial p^\nu} g_{\alpha\beta}(p') - g_{\mu\nu}(p)}{t} \\ &= \lim_{t \rightarrow 0} \frac{(\delta_\mu^\alpha + t \partial_\mu V^\alpha)(\delta_\nu^\beta + t \partial_\nu V^\beta)(g_{\alpha\beta}(p) + t V^\gamma \partial_\gamma g_{\alpha\beta}(p)) - g_{\mu\nu}(p)}{t} \\ &= g_{\alpha\nu} \partial_\mu V^\alpha + g_{\mu\beta} \partial_\nu V^\beta + V^\gamma \partial_\gamma g_{\mu\nu} \\ &= \partial_\mu V_\nu - V^\alpha \partial_\mu g_{\alpha\nu} + \partial_\nu V_\mu - V^\beta \partial_\nu g_{\mu\beta} + V^\gamma \partial_\gamma g_{\mu\nu} \\ &= \partial_\mu V_\nu + \partial_\nu V_\mu - V^\alpha (\partial_\mu g_{\alpha\nu} + \partial_\nu g_{\mu\alpha} - \partial_\alpha g_{\mu\nu}) \\ &= \partial_\mu V_\nu + \partial_\nu V_\mu - 2V_\alpha \Gamma_{\mu\nu}^\alpha \\ &= \nabla_\mu V_\nu + \nabla_\nu V_\mu = 2\nabla_{(\mu} V_{\nu)}. \end{aligned}$$

We are now ready to introduce the notion of a symmetry of spacetime $(M, g_{\mu\nu})$.

Definition 3. Let K^μ be a vector field on a (pseudo)-Riemannian manifold $(M, g_{\mu\nu})$. K^μ is called a **Killing² vector (field)** if equivalently:

¹Pronounced “Lee” after 19th century Norwegian mathematician Sophus Lie.

²After the 19th century German mathematician, Wilhelm Killing.

1. $\mathcal{L}_{K^\lambda} g_{\mu\nu} = 0$
2. $\nabla_{(\mu} K_{\nu)} \equiv \frac{1}{2}(\nabla_\mu K_\nu + \nabla_\nu K_\mu) = 0$

Killing vectors encode the symmetries of a spacetime geometry. Sometimes coordinates make it easy to find Killing vectors, as described by the following lemma.

Lemma 1. *If the components of a metric $g_{\mu\nu}$ in some particular coordinates do not depend on the coordinate k , then $(\frac{\partial}{\partial k})^\mu$ is a Killing vector field.*

Proof. Left as an exercise to the reader. \square

This leads to the main result that will help us solve the geodesic equation in Kerr.

Lemma 2. *Let $x^\mu(s)$ be a geodesic on a (pseudo)-Riemannian manifold $(M, g_{\mu\nu})$, and let K^μ be a Killing vector field, then the quantity $\mathcal{K} = K_\alpha \frac{dx^\alpha}{ds}$ is conserved along the geodesic $x^\mu(s)$.*

Proof.

$$\frac{d\mathcal{K}}{ds} = \frac{dx^\alpha}{ds} \nabla_\alpha \mathcal{K} \quad (2.2)$$

$$= \frac{dx^\alpha}{ds} \nabla_\alpha \left(K_\beta \frac{dx^\beta}{ds} \right) \quad (2.3)$$

$$= \frac{dx^\alpha}{ds} \frac{dx^\beta}{ds} \nabla_\alpha K_\beta + K_\beta \frac{dx^\alpha}{ds} \nabla_\alpha \frac{dx^\beta}{ds} \quad (2.4)$$

$$= \frac{dx^\alpha}{ds} \frac{dx^\beta}{ds} \nabla_{(\alpha} K_{\beta)} + 0 \quad (2.5)$$

$$= 0. \quad (2.6)$$

\square

The notion of a Killing vector field has a generalization to tensors for higher rank that satisfy similar properties.

Definition 4. Let $K_{\mu\nu}$ be a symmetric tensor field on a (pseudo)-Riemannian manifold $(M, g_{\mu\nu})$. $K_{\mu\nu}$ is called a **Killing tensor** (field) if

$$\nabla_{(\lambda} K_{\mu\nu)} = 0.$$

There are a number of trivial examples of Killing tensors.

Example 1. For any (pseudo)-Riemannian manifold $(M, g_{\mu\nu})$, the metric tensor itself $g_{\mu\nu}$ is a Killing tensor field.

Example 2. Suppose V^μ and W^μ are Killing vector fields, then $K_{\mu\nu} = V_{(\mu}W_{\nu)}$ is a Killing tensor.

Unlike Killing vectors, Killing tensors do not have an interpretation in terms of spacetime symmetries. Nonetheless, they still lead to constants of motion.

Lemma 3. *Let $x^\mu(s)$ be a geodesic on a (pseudo)-Riemannian manifold $(M, g_{\mu\nu})$, and let $K^{\mu\nu}$ be a Killing tensor field, then the quantity $\mathcal{K} = K_{\mu\nu} \frac{dx^\mu}{ds} \frac{dx^\nu}{ds}$ is conserved along the geodesic $x^\mu(s)$.*

Proof. Left as an exercise to the reader. □

Example 3. When applied to the metric $g_{\mu\nu}$ this lemma reproduces the familiar result that the norm of the tangent vector to a geodesic $g_{\mu\nu} \frac{dx^\mu}{ds} \frac{dx^\nu}{ds}$ is preserved along a geodesic.

2.3 Constants of Motion of Kerr geodesics

From the explicit expression for the Kerr metric in Boyer-Lindquist coordinates (1.16), we can immediately infer that the Kerr metric has two Killing vector fields $\left(\frac{\partial}{\partial t}\right)^\mu$ and $\left(\frac{\partial}{\partial \phi}\right)^\mu$, related to the time translation and axial symmetries of the spacetime, respectively. These are all the independent Killing vector fields that the Kerr metric has. (More precisely, all Killing vectors of Kerr can be written as a linear combination of $\left(\frac{\partial}{\partial t}\right)^\mu$ and $\left(\frac{\partial}{\partial \phi}\right)^\mu$).

These Killing symmetries lead to two constants of motion

$$\mathcal{E} = - \left(\frac{\partial}{\partial t} \right)_\alpha \frac{dx^\alpha}{ds} = -g_{t\alpha} \frac{dx^\alpha}{ds}, \quad (2.7)$$

$$\mathcal{L} = \left(\frac{\partial}{\partial \phi} \right)_\alpha \frac{dx^\alpha}{ds} = g_{\phi\alpha} \frac{dx^\alpha}{ds}. \quad (2.8)$$

When the affine parameter s is chosen such that $\frac{dx^\mu}{ds}$ equals the four momentum p^μ of the particle following the geodesic, \mathcal{E} is equal to the energy of the particle and \mathcal{L} is equal to the component of the orbital angular momentum along the symmetry axis of the Kerr geometry. By analogy, we will refer to \mathcal{E} and \mathcal{L} as the **energy** and **angular momentum** regardless of the chosen affine parameter.

As for any spacetime the metric $g_{\mu\nu}$ is a Killing tensor leading to our third constant of motion, the invariant mass squared

$$\mu = -g_{\mu\nu} \frac{dx^\mu}{ds} \frac{dx^\nu}{ds}. \quad (2.9)$$

It turns out that Kerr spacetime has an additional “hidden” symmetry in the form of a Killing tensor. This Killing tensor is given by

$$K_{\mu\nu} = \Sigma (\ell_\mu n_\nu + \ell_\nu n_\mu) + r^2 g_{\mu\nu}, \quad (2.10)$$

where ℓ^μ and n^ν are principal null vectors³ of the Kerr geometry. In Boyer-Lindquist coordinates their components can be written,

$$\ell^\mu = \left(\frac{r^2 + a^2}{\Delta}, 1, 0, \frac{a}{\Delta} \right), \quad \text{and} \quad (2.11)$$

$$n^\mu = \left(\frac{r^2 + a^2}{2\Sigma}, -\frac{\Delta}{2\Sigma}, 0, \frac{a}{2\Sigma} \right). \quad (2.12)$$

This gives rise to a fourth constant of motion, the **Carter constant**

$$\mathcal{K} = K_{\mu\nu} \frac{dx^\mu}{ds} \frac{dx^\nu}{ds}. \quad (2.13)$$

This constant of motion has the rough interpretation as the “total angular momentum squared” of the particle.

Any functional combination of constants of motion is also a constant of motion. It is conventional to use this freedom to replace \mathcal{K} with the constant

$$\mathcal{Q} = \mathcal{K} - (\mathcal{L} - a\mathcal{E})^2, \quad (2.14)$$

which (somewhat confusingly) is also referred to as “the Carter constant”. (We will be following this tradition.)

³This means that they are null vectors k^μ , which satisfy $k^\alpha k^\beta k_{[\mu} C_{\nu]\alpha\beta[\lambda} k_{\rho]} = 0$, which expresses that k^μ is an eigenvector of the Weyl curvature tensor $C_{\mu\nu\rho\sigma}$ in some suitable sense.

2.4 Separating the geodesic equations

So with constants of motion $(\mu, \mathcal{E}, \mathcal{L}, \mathcal{Q})$ in hand, we have four equations that a geodesic must satisfy

$$\mu = g_{\alpha\beta} \frac{dx^\alpha}{ds} \frac{dx^\beta}{ds}, \quad (2.15)$$

$$\mathcal{Q} + (\mathcal{L} - a\mathcal{E})^2 = K_{\alpha\beta} \frac{dx^\alpha}{ds} \frac{dx^\beta}{ds}, \quad (2.16)$$

$$\mathcal{E} = -g_{t\alpha} \frac{dx^\alpha}{ds}, \quad (2.17)$$

$$\mathcal{L} = g_{\phi\alpha} \frac{dx^\alpha}{ds}. \quad (2.18)$$

So, if we fix values of $(\mu, \mathcal{E}, \mathcal{L}, \mathcal{Q})$, we have four equations for four unknowns (the components of $\frac{dx^\mu}{ds}$), and we can solve these equations. After some straightforward (but tedious) algebra we find

$$\left(\frac{dr}{ds}\right)^2 = \frac{(\mathcal{E}(r^2 + a^2) - a\mathcal{L})^2 - \Delta(\mathcal{Q} + (\mathcal{L} - a\mathcal{E})^2 + \mu r^2)}{\Sigma^2} \quad (2.19)$$

$$\left(\frac{d\cos\theta}{ds}\right)^2 = \frac{\mathcal{Q} - \cos^2\theta(a^2(\mu - \mathcal{E}^2)\sin^2\theta + \mathcal{L}^2 + \mathcal{Q})}{\Sigma^2} \quad (2.20)$$

$$\frac{dt}{ds} = \frac{\frac{r^2+a^2}{\Delta}(\mathcal{E}(r^2 + a^2) - a\mathcal{L}) - a^2\mathcal{E}\sin^2\theta + a\mathcal{L}}{\Sigma}, \text{ and} \quad (2.21)$$

$$\frac{d\phi}{ds} = \frac{\frac{a}{\Delta}(\mathcal{E}(r^2 + a^2) - a\mathcal{L}) + \frac{\mathcal{L}}{\sin^2\theta} - a\mathcal{E}}{\Sigma}. \quad (2.22)$$

This is already a huge improvement over the general geodesic equations in that only first order derivatives appear. Moreover, t and ϕ do not appear at all on the right hand side of the equations. If we can manage to solve the equations for r and θ the solutions for t and ϕ can be found by direct integration. Finally, the equations for r and θ appear almost entirely decoupled, apart from the Σ in the denominators the right hand side of the radial (r) equation depends only on r and the polar (θ) equation depends only on θ . Having decoupled equations would be nice since we could then solve each equation independently. To fully decouple the equations we introduce a new time parameter, the **Mino-Carter time** λ defined by

$$\frac{d\lambda}{ds} = \frac{1}{\Sigma}. \quad (2.23)$$

With this choice our equations become

$$\begin{aligned}
\left(\frac{dr}{d\lambda}\right)^2 &= (\mathcal{E}(r^2 + a^2) - a\mathcal{L})^2 - \Delta(\mathcal{Q} + (\mathcal{L} - a\mathcal{E})^2 + \mu r^2) = P_r(r) \\
\left(\frac{d\cos\theta}{d\lambda}\right)^2 &= \mathcal{Q} - \cos^2\theta(a^2(\mu - \mathcal{E}^2)\sin^2\theta + \mathcal{L}^2 + \mathcal{Q}) = P_\theta(\cos\theta) \\
\frac{dt}{d\lambda} &= \frac{r^2 + a^2}{\Delta}(\mathcal{E}(r^2 + a^2) - a\mathcal{L}) - a^2\mathcal{E}\sin^2\theta + a\mathcal{L} = T_r(r) + T_\theta(\cos\theta) \\
\frac{d\phi}{d\lambda} &= \frac{a}{\Delta}(\mathcal{E}(r^2 + a^2) - a\mathcal{L}) + \frac{\mathcal{L}}{\sin^2\theta} - a\mathcal{E} = \Phi_r(r) + \Phi_\theta(\cos\theta).
\end{aligned}$$

These equations are completely decoupled. Moreover, the right hand side of the t and ϕ equations separate as the sum of something that depends on r with something that depends on θ . Consequently, these can be integrated separately for different radial and polar solutions.

The equations for r and $\cos\theta$ each individually take the form of a particle moving in a 1-dimensional potential. The functions P_r and P_θ are therefore known as the **radial** and **polar potentials**. Note that instead of the equations involving the square of the first derivatives (for r and θ) we can easily return to second order differential equations (which now will also be decoupled) by taking the derivative with respect to λ to yield

$$\frac{d^2r}{d\lambda^2} = \frac{1}{2}P'_r(r), \quad \text{and} \quad (2.24)$$

$$\frac{d^2\cos\theta}{d\lambda^2} = \frac{1}{2}P'_\theta(\cos\theta). \quad (2.25)$$

2.5 The polar equation

$$\left(\frac{d\cos\theta}{d\lambda}\right)^2 = \mathcal{Q} - \cos^2\theta(a^2(\mu - \mathcal{E}^2)\sin^2\theta + \mathcal{L}^2 + \mathcal{Q}) = P_\theta(\cos\theta) \quad (2.26)$$

Because the left-hand side of the equation is a square, we can only find solutions if the right-hand side is not negative, i.e. when $P_\theta(\cos\theta) \geq 0$. We can therefore learn about the possible solutions by studying the roots of the polynomial $P_\theta(z)$. Since $P_\theta(z)$ is a fourth order polynomial in $z = \cos\theta$, there at most 4 real roots. Moreover, since $P_\theta(z)$ is an even function of z these roots come in pairs $z = \pm z_i$. Consequently,

$$P_\theta(z) = a^2(\mu - \mathcal{E}^2)(z^2 - z_1^2)(z^2 - z_2^2). \quad (2.27)$$

If we evaluate $P_\theta(z)$ at the poles $z = \pm 1$, we find that $P_\theta(\pm 1) = -\mathcal{L}^2$. We thus immediately learn geodesics can only reach the poles when $\mathcal{L} = 0$.

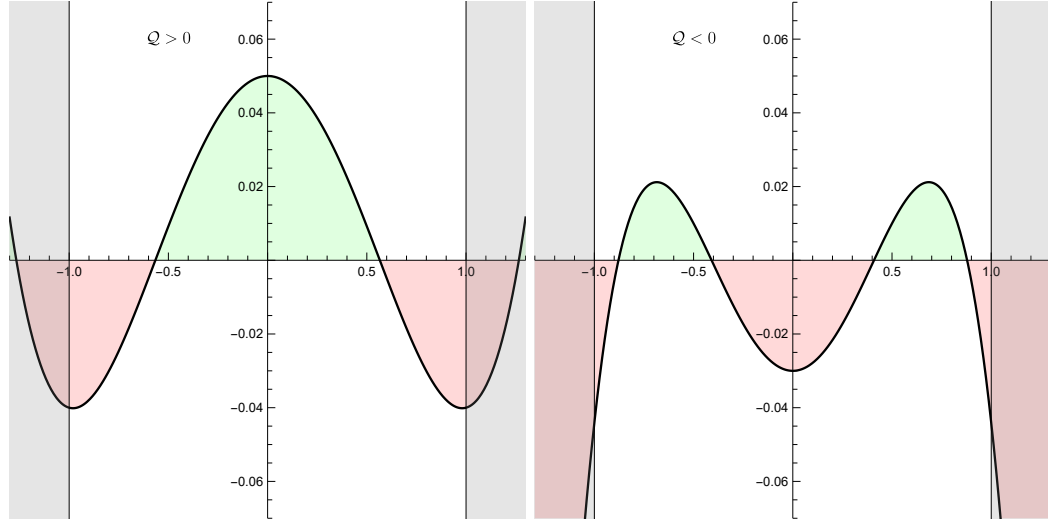


Figure 2.1: The polar potential P_θ when \mathcal{Q} is positive (on the left) or negative (on the right). In the positive \mathcal{Q} case, we find solutions where $\cos \theta$ oscillates around the equator ($\cos \theta = 0$) between $\pm z_1$. In the negative \mathcal{Q} case, we can get vortical solutions where $\cos \theta$ oscillates between $z_1 < z_2$ (or $-z_2 < -z_1$), but never crosses the equator.

When we evaluate $P_\theta(z)$ on the equator $\cos \theta = 0$ we find that $P_\theta(0) = \mathcal{Q}$. Therefore, we only find solutions that visit the equator when $\mathcal{Q} \geq 0$. If $\mathcal{Q} > 0$ and $\mathcal{L} \neq 0$, there must be an odd number of zeroes between 0 and 1, and the same number between -1 and 0. Since there are at most 4 zeroes, there is exactly one such zero z_1 , and the only solutions oscillate around the equator between $\pm z_1$. In the Schwarzschild ($a \rightarrow 0$) limit, these solutions describe trajectories whose orbital plane is inclined relative to the equator of the coordinate system. As such these solutions are generally known as **inclined** trajectories. In Kerr this orbital plane precesses, leading to another common name **precessing** trajectories.

If $\mathcal{Q} = 0$, then $z = 0$ is a double root of P_θ . This implies that $x = \cos \theta = 0$ is constant is a solution to the differential equation. These solutions stay in the Kerr equatorial plane and are therefore known as **equatorial** trajectories.

If $\mathcal{Q} < 0$ then no solution is possible near the equator. In this case, it is only possible for P_θ to be positive somewhere in the range $-1 < \cos \theta < 1$, if P_θ has exactly two zeroes $0 < z_1 < z_2 \leq 1$. We can easily see that this is only possible if $\mu < \mathcal{E}^2$ by considering the behavior of P_θ at large z . At large z , $P_\theta = a^2(\mu - \mathcal{E}^2)z^4 + \mathcal{O}(z^2)$. So, if $\mu > \mathcal{E}^2$ the polar potential becomes positive at large z . Consequently, there must be at least one zero between $z = 1$ (where P_θ is negative) and $z = \infty$, and there cannot be four roots in

Type	$\mu - \mathcal{E}^2$	$\frac{\mathcal{L}^2}{a^2(\mathcal{E}^2 - \mu)}$	\mathcal{Q}	$z = \cos \theta$
Equatorial	any	any	0	0
Inclined	any	any	> 0	$-z_1 < z < z_1$
Vortical	< 0	≤ 1	$-1 \leq \frac{\mathcal{Q}}{(\mathcal{L} - a \sqrt{\mathcal{E}^2 - \mu})^2} \leq 0$	$z_1 < z < z_2$

Table 2.1: Classification of solutions of the polar equation.

the range $-1 < z < 1$. The condition $\mu < \mathcal{E}^2$ is by itself not sufficient the existence of two zeroes $0 < z_1 < z_2 \leq 1$. One can show (but we will not here) that such roots exist if and only if the following conditions are met

$$\mathcal{L}^2 \leq a^2(\mathcal{E}^2 - \mu) \text{ and } -\left(|\mathcal{L}| - |a|\sqrt{\mathcal{E}^2 - \mu}\right)^2 \leq \mathcal{Q} \leq 0. \quad (2.28)$$

Solutions of this type are referred to as **vortical** trajectories.

2.6 The radial equation

The decoupled equation for radial motion is given by

$$\left(\frac{dr}{d\lambda}\right)^2 = (\mathcal{E}(r^2 + a^2) - a\mathcal{L})^2 - \Delta(\mathcal{Q} + (\mathcal{L} - a\mathcal{E})^2 + \mu r^2) = P_r(r). \quad (2.29)$$

It has the same, overall structure as the polar equation. In particular, we can only have solutions when the radial potential P_r is non-negative, and the radial potential is a fourth order polynomial in r , which therefore has four zeroes r_i (0, 2, or 4 of which may be real-valued) and can be written

$$P_r = (\mathcal{E}^2 - \mu)(r - r_1)(r - r_2)(r - r_3)(r - r_4). \quad (2.30)$$

As with the polar equation it will be useful to examine the value of P_r at specific values of r . We start with $r = 0$, and observe that $P_r(0) = -a^2\mathcal{Q}$. Consequently, solutions to the radial equation can only reach $r = 0$ if $\mathcal{Q} \leq 0$, i.e. only equatorial and vortical trajectories can ever reach $r = 0$. Of these, only the equatorial ($\mathcal{Q} = 0$) solutions can ever reach the curvature singularity at $\theta = \pi/2$. We thus find that of all geodesics in Kerr only a measure zero subset hit the singularity. All others miss it entirely, some of them passing through the ring singularity to the $r < 0$ region (all of them vortical) and some of them scattering back due to centrifugal barrier.

Next we turn our attention to the horizon r_{\pm} , since Δ vanishes here we find

$$P_r = (\mathcal{E}(r_{\pm}^2 + a^2) - a\mathcal{L})^2 \geq 0. \quad (2.31)$$

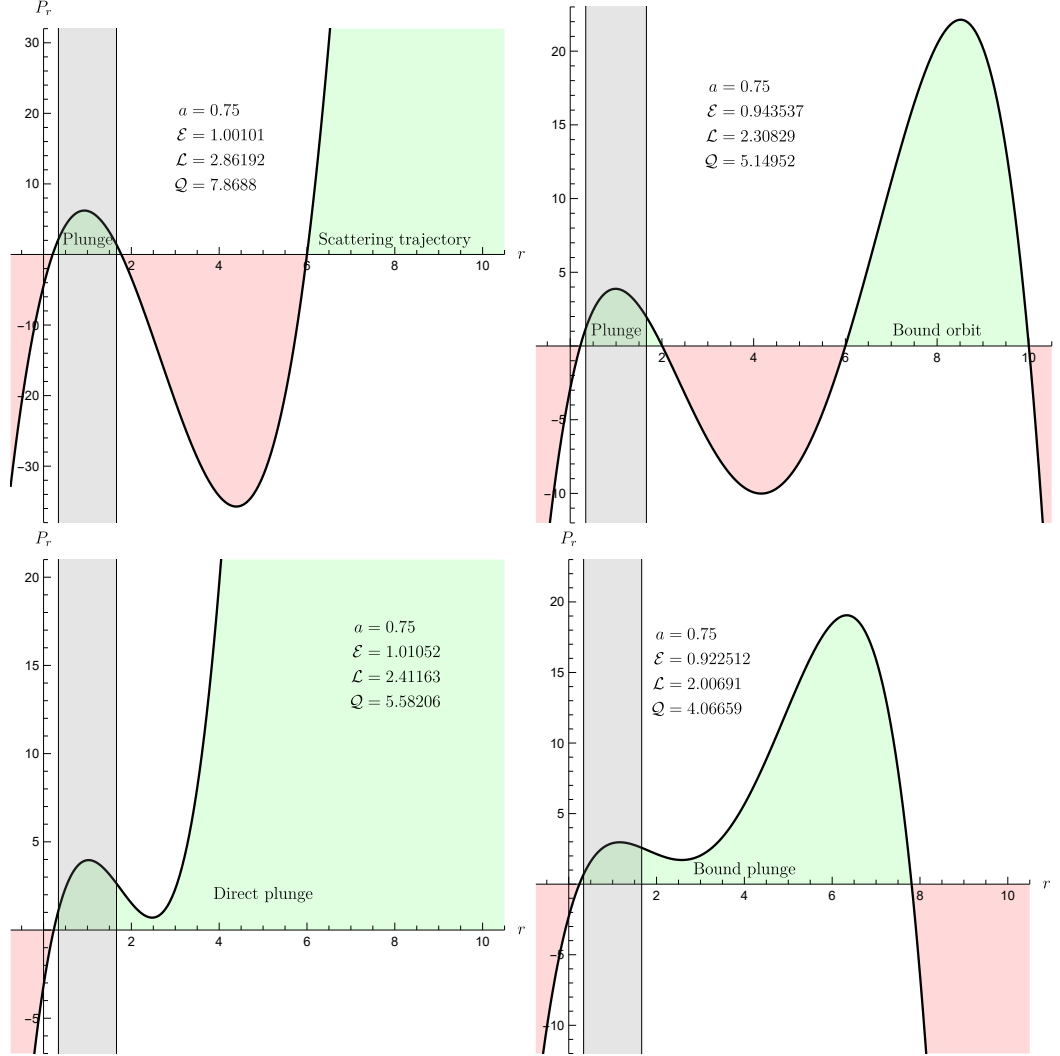


Figure 2.2: The radial potential P_r for a scattering trajectory (top left), bound orbit (top right), direct plunge (bottom left), and bound plunge (bottom right). Note the existence of secondary “deeply bound” plunge solutions in the top plots.

Consequently, for all values of $(\mu, \mathcal{E}, \mathcal{L}, \mathcal{Q})$ that allow the existence of solutions to the polar equation, we have solutions that cross the horizons. Moreover, since r is timelike between the horizons, we cannot have any zeroes between r_{\pm} for timelike $\mu > 0$ and null $\mu = 0$ solutions. This also implies that if $\mathcal{Q} > 0$ then there must exist at least one (and at most three) zeroes between the inner horizon r_- and $r = 0$.

Last we turn our attention to the behavior of P_r as r approaches $\pm\infty$. Expand P_r we find $P_r = (\mathcal{E}^2 - \mu)r^4 + \mathcal{O}(r^3)$. Consequently, in order for a geodesic to reach infinity $(\mathcal{I}^{\pm}, i^{\pm}, i^0)$ it must have $\mathcal{E}^2 > \mu$. For this reason geodesics satisfying this condition are referred to as **unbound**. Note that for null geodesics $\mu = 0$; they are necessarily unbound.

For unbound $\mathcal{E}^2 > \mu$ geodesics the radial potential must have an even number of zeroes between the outer horizon r_+ and $r = \infty$. When there no zeroes in this region the solution corresponds to a trajectory that starts at infinity and dives directly into the black hole. These solutions are known as **direct plunges**.

If there are two zeroes $r_1 > r_2$ in the region outside of the black hole, solutions correspond to trajectories starting from infinity, and scattering of the black hole potential back to infinity. These trajectories are known as **scattering** or **hyperbolic** trajectories.

Geodesics with $\mathcal{E}^2 < \mu$ are only possible for timelike trajectories with $\mu > 0$, and known as **bound** trajectories because they do not possess enough energy to reach infinity. The existence of a polar solution implies that for bound orbits we necessarily have that $\mathcal{Q} \geq 0$, and therefore that there exists at least one zero inside the inner horizon. Since the radial potential changes sign between the outer horizon r_+ and infinity there must be either one or three zeroes outside the outer horizon.

If there exists just one zero $r_+ < r_1 < \infty$ the solution corresponds to a trajectory starting at the past horizon moving outward to r_1 and then diving back into the black hole. These trajectories are known as **(bound) plunges**. Of course, these geodesics do not stop at the horizon. If followed into the black hole, they will also cross the inner horizon before encountering a turning point in the inner region, and proceeding back outward through the inner horizon and exiting the outer horizon into a new parallel universe in the maximally extended Kerr solution, after which the above repeats ad infinitum with the geodesic eventually (according to its own proper time) visiting infinitely many copies of the external universe.

If there are three zeroes $r_+ < r_3 < r_2 < r_1 < \infty$ then the solution oscillates between r_1 and r_2 to form a **bound (eccentric) orbit**.

Note that both in the case of bound orbits and scattering orbits, there exists a secondary solution with the same constants of motion which oscillates

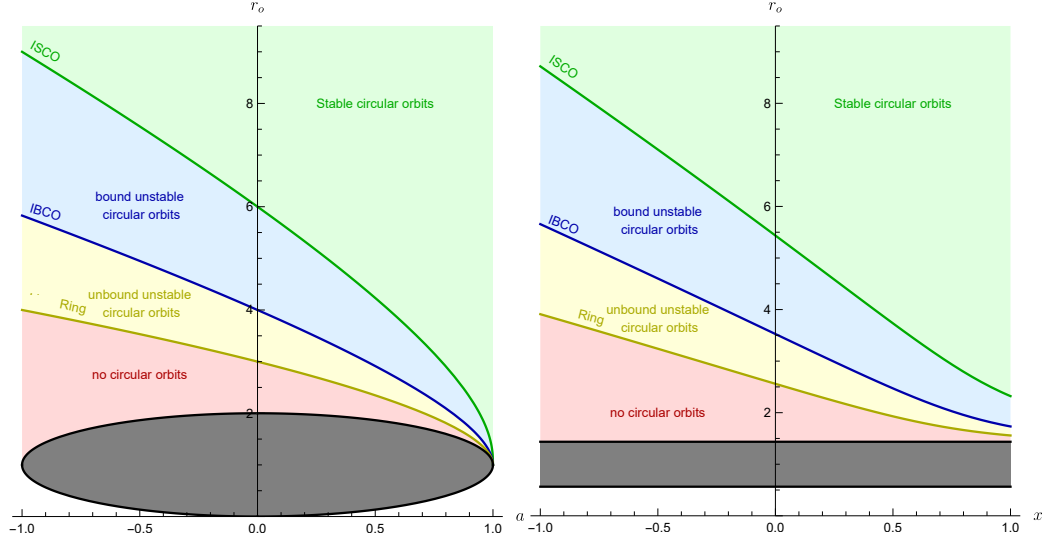


Figure 2.3: The location of the ISCO, IBCO, and light ring in Kerr. On the left, equatorial orbits, on the right at fixed spin $a = 0.9M$.

between the remaining turning point outside the horizon and the zero inside the inner horizon (if $\mathcal{Q} > 0$). These solutions behave similarly to the bound plunges and are therefore known as **deeply bound plunges**.

2.6.1 Circular orbits

Circular orbits are geodesics for which the radial potential allows a constant solution r_o . This requires not only that $P_r(r_o) = 0$ (which ensures that $\frac{dr}{d\lambda} = 0 = \frac{dr}{ds}$), but also that $P'_r(r_o) = 0$ (which ensures that $\frac{d^2r}{d\lambda^2} = 0 = \frac{d^2r}{ds^2}$). This therefore requires that r_o is a double zero of the radial potential. A double zero can be either a maximum or minimum of the radial potential. In the former case the circular orbit is **stable**; any small perturbation will produce an eccentric orbit with small eccentricity. In the latter case, the circular orbit is **unstable**; any perturbation leads to a wildly different orbit.

Stable circular orbits occur as the limit of eccentric orbits as the zeroes r_1 and r_2 merge. Unstable circular orbits are formed by merging the inner turning point of a scattering or bound orbit with the outer turning point of a deeply bound plunge.

Stable circular orbits can only be found outside a certain radius, the **innermost stable circular orbit** or **ISCO**. Inside this radius one can still find circular orbits, but they become increasingly unstable with larger and larger energies. Initially, these unstable circular orbits have low enough

energies, that even after a perturbation the particle will stay bound to the black hole. However, below another radius, the **innermost bound circular orbit** or **IBCO**, the energy becomes large enough that perturbations can send the particle scattering to infinity. Finally, the energy of the circular orbits diverges at the **light ring**, this radius can only be approached if one simultaneously allows the mass μ to go to zero, and the geodesic to become null. Inside the light ring no circular orbits are possible (outside the event horizon).

2.7 Characterizing bound orbits

In the previous sections we have found the bound orbits ($\mu > \mathcal{E}^2$) are necessarily either inclined ($\mathcal{Q} > 0$) or equatorial ($\mathcal{Q} = 0$), and corresponds a solution oscillating in the radial direction between $r_1 \geq r_2 > r_+$, and in the polar direction between $\pm z_1$. There are a number of characterizations of these orbits that useful in identifying them

- The **constants of motion** ($\mathcal{E}, \mathcal{L}, \mathcal{Q}$). For any sets of values of the constants of motion, if a bound orbit exists then that solution is unique. (There will always also exist a deeply bound plunge with the same constants of motion.)
- The **turning points** (r_1, r_2, z_1) uniquely characterize a bound orbit up to the direction of motion: with the rotation of the black hole (**prograde**) or against the rotation of the black hole (**retrograde**). This degeneracy is conventionally broken by the convention that the angular momentum \mathcal{L} is always positive, and letting the sign of the spin determine the sense of the motion. The turning point r_1 is known as the **apocenter** and r_2 as the **pericenter**.
- A Keplerian-like parametrization consting of the

$$\begin{aligned}
 p &= \frac{2r_1 r_2}{r_1 + r_2} && \text{semi-latus rectum} \\
 e &= \frac{r_1 - r_2}{r_1 + r_2} && \text{eccentricity} \\
 x &= \begin{cases} \sqrt{1 - z_1^2} & \text{prograde} \\ -\sqrt{1 - z_1^2} & \text{retrograde} \end{cases} && \text{inclination}
 \end{aligned}$$

In this parametrization $e = 0$ corresponds to circular motion, and $x = \pm 1$ corresponds to equatorial motion.

- A more phenomenological characterization is in terms of **periods** of orbit
 - Λ_r The (Mino time) period of the radial motion.
 - Λ_θ The (Mino time) period of the polar motion.
 - Λ_ϕ The average Mino time needed to complete an orbital cycle.

The triple $(\Lambda_r, \Lambda_\theta, \Lambda_\phi)$, uniquely identifies a (relativistic) bound orbit. This may come as surprise to those familiar of Newtonian orbital dynamics where we always have $\Lambda_r = \Lambda_\theta = \Lambda_\phi$.

- Similarly, the **Mino time frequencies**

$$\begin{aligned}\Upsilon_r &= \frac{2\pi}{\Lambda_r} \\ \Upsilon_\theta &= \frac{2\pi}{\Lambda_\theta} \\ \Upsilon_\phi &= \frac{2\pi}{\Lambda_\phi} = \lim_{\Lambda \rightarrow \infty} \frac{1}{2\Lambda} \int_{-\Lambda}^{\Lambda} \frac{d\phi}{d\lambda} d\lambda.\end{aligned}$$

In the same spirit as the azimuthal frequency we can define the average advance of the Boyer-Lindquist time t ,

$$\Upsilon_t = \lim_{\Lambda \rightarrow \infty} \frac{1}{2\Lambda} \int_{-\Lambda}^{\Lambda} \frac{dt}{d\lambda} d\lambda.$$

This allows us to define the **Boyer-Lindquist frequencies** of the orbit.

$$\begin{aligned}\Omega_r &= \frac{\Upsilon_r}{\Upsilon_t} \\ \Omega_\theta &= \frac{\Upsilon_\theta}{\Upsilon_t} \\ \Omega_\phi &= \frac{\Upsilon_\phi}{\Upsilon_t}.\end{aligned}$$

The Boyer-Lindquist frequencies are frequencies that a distant observer at rest would infer when observing the system. Unlike the Mino-time frequencies the triple $(\Omega_r, \Omega_\theta, \Omega_\phi)$ does not always uniquely identify a bound orbit. In the strong field regime, we typically encounter pairs of distinct **isofrequency** orbits with the same Boyer-Lindquist frequencies.

Two other commonly observed quantities are :

- The **pericenter advance** $\Upsilon_\phi \Lambda_r - 2\pi$

- The **nodal advance** $\Upsilon_\phi \Lambda_\theta - 2\pi$

Although we are not going to derive them here, explicit expressions for all these quantities (and the corresponding geodesic solutions) can be obtained analytically by solving the ODEs. These solutions can be obtained e.g. from the Black Hole Perturbation Toolkit [1].

2.8 Null geodesics and black hole shadows

Null geodesics describe the trajectories of light rays through the spacetime. From the analysis in the previous sections we note that setting $\mu = 0$ implies that null geodesics are always unbound. As observers far away from a typical black hole we are interested in light rays that can reach as at infinity. We found that there is two main possibilities if we follow such a ray back in time either:

- The ray follows a scattering trajectory with $r \geq r_2 \geq r_3 > r_+$. In this case the polar motion must be either equatorial or inclined.

or

- The ray follows a (time reversed) direct plunge originating from the past horizon (with no zeroes outside the horizon). In this case the polar motion can be any of equatorial, inclined, or vortical.

More coming...

Chapter 3

Black Hole Perturbation Theory

3.1 Perturbation theory in GR

Globally speaking, when applying perturbation theory to general relativity we want to make the statement that some given spacetime $(M, g_{\mu\nu})$ is equal to some background spacetime $(\bar{M}, \bar{g}_{\mu\nu})$ plus something “small”. However, the equation

$$(M, g_{\mu\nu}) = (\bar{M}, \bar{g}_{\mu\nu}) + \text{“something small”}$$

doesn’t really make much mathematical sense. To make sense of such a comparison we will need a map $\phi : \bar{M} \rightarrow M$ that identifies the points of \bar{M} with those of M . This makes it possible to compare any tensors (such as the metric) that “live” on M with tensors that live in \bar{M} by considering the pull back of the object. E.g. we can consider the difference between the pull-back of $g_{\mu\nu}$ and compare it with $\bar{g}_{\mu\nu}$

$$\delta_\phi g_{\mu\nu} = \phi^* g_{\mu\nu} - \bar{g}_{\mu\nu},$$

and ask ourselves whether this is small. However, we should now wonder how this comparison depends on the choice of ϕ . What would change if we had chosen a different map $\varphi : \bar{M} \rightarrow M$ identify the points of \bar{M} and M ? To answer this question note that if ϕ and φ are both diffeomorphisms then there exists a unique automorphism $\psi : \bar{M} \rightarrow \bar{M}$ such that $\varphi = \phi \circ \psi$, which is generated by some vector field ξ^μ .

To compare $\delta_\phi g_{\mu\nu}$ and $\delta_\varphi g_{\mu\nu}$ we first note that starting from the same image point $p \in M$, the differences $\delta_\varphi g_{\mu\nu}$ and $\delta_\phi g_{\mu\nu}$ “live” at difference points

$\bar{p}, \bar{p}' \in \bar{M}$ satisfying $\bar{p}' = \psi(\bar{p})$. So to compare the two we need to pullback $\delta_\phi g_{\mu\nu}$ to \bar{p} using ψ^* . In the limit that ξ^μ is small we get

$$\begin{aligned}
\delta_\phi g_{\mu\nu} - \psi^* \delta_\phi g_{\mu\nu} &= \varphi^* g_{\mu\nu} - \bar{g}_{\mu\nu} - \psi^*(\phi^* g_{\mu\nu} - \bar{g}_{\mu\nu}) \\
&= (\phi \circ \psi)^* g_{\mu\nu} - \bar{g}_{\mu\nu} - \psi^*(\phi^* g_{\mu\nu} - \bar{g}_{\mu\nu}) \\
&= \psi^* \phi^* g_{\mu\nu} - \bar{g}_{\mu\nu} - \psi^* \phi^* g_{\mu\nu} + \psi^* \bar{g}_{\mu\nu} \\
&= \psi^* \bar{g}_{\mu\nu} - \bar{g}_{\mu\nu} \\
&= \mathcal{L}_{\xi^\mu} \bar{g}_{\mu\nu} + \mathcal{O}(\xi^2) \\
&= \nabla_\mu \xi_\nu + \nabla_\nu \xi_\mu + \mathcal{O}(\xi^2)
\end{aligned}$$

So, fundamentally the comparison of $g_{\mu\nu}$ with $\bar{g}_{\mu\nu}$ is ambiguous up to a Lie derivative of $\bar{g}_{\mu\nu}$. In to context of perturbation theory this is known as a **gauge** ambiguity. More generally, when comparing any tensor $T_{\mu_1 \dots \mu_n}$ with a background tensor $\bar{T}_{\mu_1 \dots \mu_n}$ that comparison has a gauge ambiguity $\mathcal{L}_{\xi^\mu} \bar{T}_{\mu_1 \dots \mu_n}$.

Lemma 4. *If a background tensor $\bar{T}_{\mu_1 \dots \mu_n}$ is zero, then its perturbations are free from gauge ambiguities. A quantity free from gauge ambiguities is called ***gauge invariant***.*

Note that this gauge freedom in perturbation theory is logically distinct from the general coordinate freedom of general relativity. However, in practice the two are closely related, since we tend to construct the identification map ϕ by choosing similar coordinates on \bar{M} and M and identifying the points with the same coordinate values. Consequently, the ambiguity ψ in this identification map simply becomes the ambiguity of choosing the coordinates.

Moving forward we will drop the fancy notation involving identification maps, and work with the understanding that a suitably identification map has been chosen and used to pull back all tensors to the background manifold \bar{M} . Consequently, all tensors will be tensors on the manifold \bar{M} and all raising and lowering operations are understood to use the background metric $\bar{g}_{\mu\nu}$. Moreover, any perturbations are understood as being ambiguous up to gauge transformations defined by gauge vectors ξ^μ

Using these conventions we are now ready to write that

$$g_{\mu\nu} = \bar{g}_{\mu\nu} + \epsilon h_{\mu\nu} + \mathcal{O}(\epsilon^2)$$

where $h_{\mu\nu}$ is a symmetric rank-2 tensor living on \bar{M} known as the (first-order) **metric perturbation**, and $\epsilon > 0$ is a small number that we will use to keep track of the orders in our perturbation theory. The metric perturbations are ambiguous up to transformations

$$h_{\mu\nu} \mapsto h_{\mu\nu} + \nabla_\mu \xi_\nu + \nabla_\nu \xi_\mu.$$

We can try to fix this gauge freedom by imposing additional conditions on $h_{\mu\nu}$.

So, suppose now we want to know what the inverse perturbed metric $g^{\mu\nu}$ looks like. Note $g^{\mu\nu}$ is now considered a tensor of \bar{M} , but cannot be obtained by simply raising the indices on $g_{\mu\nu}$. We should therefore be using a different symbol. Let's write

$$g^{\mu\nu} = A^{\mu\nu} + \epsilon B^{\mu\nu} + \mathcal{O}(\epsilon^2).$$

The inverse metric will still have to satisfy

$$\delta_\mu{}^\nu = g_{\mu\alpha} g^{\alpha\nu} = (\bar{g}_{\mu\alpha} + \epsilon h_{\mu\alpha})(A^{\alpha\nu} + \epsilon B^{\alpha\nu}) = \bar{g}_{\mu\alpha} A^{\alpha\nu} + \epsilon(h_{\mu\alpha} A^{\alpha\nu} + \bar{g}_{\mu\alpha} B^{\alpha\nu}) + \mathcal{O}(\epsilon^2)$$

This equation will have to be satisfied order-by-order in ϵ . Giving us

$$\begin{aligned} \delta_\mu{}^\nu &= \bar{g}_{\mu\alpha} A^{\alpha\nu}, \quad \text{and} \\ 0 &= h_{\mu\alpha} A^{\alpha\nu} + \bar{g}_{\mu\alpha} B^{\alpha\nu}, \end{aligned}$$

which we can solve to find

$$g^{\mu\nu} = \bar{g}^{\mu\nu} - \epsilon h^{\mu\nu} + \mathcal{O}(\epsilon^2)$$

.

3.2 Linearized Einstein Equation

Literature: Wald Sec. 7.5

We now want to make our way to the perturbed form of the Einstein equation. For this we first observe that both ∇_μ and $\bar{\nabla}_\mu$ are covariant derivatives, but compatible with different metrics. Consequently, we have that their difference

$$(\nabla_\mu - \bar{\nabla}_\mu) V^\nu = (\Gamma_{\mu\alpha}^\nu - \bar{\Gamma}_{\mu\alpha}^\nu) V^\alpha = \epsilon C_{\mu\alpha}^\nu V^\alpha$$

is represented by a rank 3-tensor $C_{\mu\alpha}^\nu$.

Equivalently, we could express this as

$$\nabla_\mu V^\nu = \bar{\nabla}_\mu V^\nu + \epsilon C_{\mu\alpha}^\nu V^\alpha.$$

This is similar to the usual expression for the covariant derivative, but with the partial derivative replaced by the background covariant derivative and the Christoffel symbols $\Gamma_{\mu\alpha}^\nu$ replaced by the tensor $C_{\mu\alpha}^\nu$.

Compatibility, of ∇_μ with the metric $g_{\mu\nu}$, yields an expression for $C^\nu_{\mu\alpha}$ in the same way we obtained our expression for the Christoffel symbols of the Levi-Civita connection (see e.g. Theorem 3.1.1 in Wald)

$$\begin{aligned}\epsilon C^\lambda_{\mu\nu} &= \frac{1}{2} g^{\lambda\alpha} (\bar{\nabla}_\mu g_{\nu\alpha} + \bar{\nabla}_\nu g_{\alpha\mu} - \bar{\nabla}_\alpha g_{\mu\nu}) \\ &= \epsilon \frac{1}{2} \bar{g}^{\lambda\alpha} (\bar{\nabla}_\mu h_{\nu\alpha} + \bar{\nabla}_\nu h_{\alpha\mu} - \bar{\nabla}_\alpha h_{\mu\nu}) + \mathcal{O}(\epsilon^2).\end{aligned}$$

The Riemann tensor will now be given

$$R^\lambda_{\sigma\mu\nu} = \bar{R}^\lambda_{\sigma\mu\nu} + \epsilon (\bar{\nabla}_\mu C^\lambda_{\nu\sigma} - \bar{\nabla}_\nu C^\lambda_{\mu\sigma}) + \epsilon^2 (C^\lambda_{\mu\alpha} C^\alpha_{\nu\sigma} - C^\lambda_{\nu\alpha} C^\alpha_{\mu\sigma}).$$

The Einstein equation can be written

$$R_{\mu\nu} = 8\pi \left(T_{\mu\nu} - \frac{1}{2} g_{\mu\nu} T \right),$$

where $T = g^{\alpha\beta} T_{\alpha\beta}$ the trace of the energy-momentum tensor. Lets assume we are expanding around a background metric $\bar{g}_{\mu\nu}$ that is itself a solutions to the vacuum Einstein equation (e.g. Kerr), such that $\bar{R}_{\mu\nu} = 0$. We then find

$$\begin{aligned}R_{\mu\nu} &= R^\alpha_{\mu\alpha\nu} \\ &= \epsilon (\bar{\nabla}_\alpha C^\alpha_{\mu\nu} - \bar{\nabla}_\nu C^\alpha_{\alpha\mu}) + \mathcal{O}(\epsilon^2) \\ &= \frac{\epsilon}{2} \bar{g}^{\alpha\beta} (\bar{\nabla}_\alpha (\bar{\nabla}_\mu h_{\nu\beta} + \bar{\nabla}_\nu h_{\beta\mu} - \bar{\nabla}_\beta h_{\mu\nu}) \\ &\quad - \bar{\nabla}_\nu (\bar{\nabla}_\alpha h_{\mu\beta} + \bar{\nabla}_\mu h_{\beta\alpha} - \bar{\nabla}_\beta h_{\alpha\mu})) + \mathcal{O}(\epsilon^2) \\ &= \frac{\epsilon}{2} (-\bar{\square} h_{\mu\nu} - \bar{\nabla}_\nu \bar{\nabla}_\mu h + 2 \bar{\nabla}^\alpha \bar{\nabla}_{(\mu} h_{\nu)\alpha}) + \mathcal{O}(\epsilon^2) \\ &= \frac{\epsilon}{2} (-\bar{\square} h_{\mu\nu} - \bar{\nabla}_\nu \bar{\nabla}_\mu h + 2 \bar{\nabla}_{(\mu} \bar{\nabla}^\alpha h_{\nu)\alpha} + 2 \bar{R}^\alpha_{\mu\nu}{}^\beta h_{\alpha\beta}) + \mathcal{O}(\epsilon^2),\end{aligned}$$

where $\bar{\square} = \bar{\nabla}^\alpha \bar{\nabla}_\alpha$, and $h = h_{\alpha\beta} \bar{g}^{\alpha\beta}$ is the trace of the metric perturbation, and in the last line we used that $\bar{\nabla}_\mu \bar{\nabla}_\nu h_{\alpha\beta} = \bar{\nabla}_\nu \bar{\nabla}_\mu h_{\alpha\beta} + \bar{R}_{\mu\nu\beta}{}^\gamma h_{\alpha\gamma} + \bar{R}_{\mu\nu\alpha}{}^\gamma h_{\gamma\beta}$. Moreover, since the background was vacuum the energy momentum tensor $T_{\mu\nu}$ must also be order ϵ . Consequently, the order ϵ of the Einstein equation becomes,

$$\frac{1}{2} \bar{\square} h_{\mu\nu} + \frac{1}{2} \bar{\nabla}_{(\mu} \bar{\nabla}_{\nu)} h - \bar{\nabla}_{(\mu} \bar{\nabla}^\alpha h_{\nu)\alpha} - \bar{R}^\alpha_{\mu\nu}{}^\beta h_{\alpha\beta} = -8\pi \left(T_{\mu\nu} - \frac{1}{2} \bar{g}_{\mu\nu} T \right). \quad (3.1)$$

We can further simplify this by using the gauge freedom in the metric perturbation. By choosing the Lorenz¹ gauge condition

$$\bar{\nabla}^\alpha h_{\mu\alpha} = \frac{1}{2} \bar{\nabla}_\mu h, \quad (3.2)$$

¹After the 19th century Danish physicist Ludvig Lorenz, not the 19th century Dutch physicist Hendrik Lorentz.

the linearized Einstein equation becomes

$$\frac{1}{2}\square h_{\mu\nu} - \bar{R}^{\alpha}{}_{\mu\nu}{}^{\beta} h_{\alpha\beta} = -8\pi \left(T_{\mu\nu} - \frac{1}{2}\bar{g}_{\mu\nu}T \right). \quad (3.3)$$

In this gauge, the linearized Einstein equation explicitly takes the form of a wave equation. However, we should not be deceived by the apparent simplicity of this equation, it still consists of 10 coupled second order partial differential equations, and solving them is generally hard. Sometimes, the symmetries of the background help. For example, for a Schwarzschild background the equations can be solved through separation of variables, allowing the solution to be found mode-by-mode. For each mode, it then reduces to a set of 10 coupled ordinary differential equations. But even in Kerr, there is no known way to separate the variables.

It is therefore worth to consider a different approach.

3.3 The Penrose Wave Equation

Instead of a wave equation for the metric we will pursue a wave equation for the curvature instead. The Riemann curvature tensor $R_{\mu\nu\alpha\beta}$ in 4 dimensions has 20 degrees of freedom. Ten of these are encoded by the Ricci tensor $R_{\mu\nu} = R^{\alpha}{}_{\mu\alpha\nu}$, which through the Einstein equation are algebraically determined by the energy-momentum content. The remaining 10 degrees of freedom are captured by the trace-free part of the Riemann tensor, the so-called Weyl tensor

$$C_{\mu\nu\alpha\beta} = R_{\mu\nu\alpha\beta} - g_{\alpha[\mu}R_{\nu]\beta} + g_{\beta[\mu}R_{\nu]\alpha} + \frac{R}{3}g_{\alpha[\mu}g_{\nu]\beta}. \quad (3.4)$$

It is defined in such a way that any contraction of its indices produces zero, while retaining the symmetries of $R_{\mu\nu\alpha\beta}$,

$$C_{\mu\nu\alpha\beta} = C_{[\mu\nu][\alpha\beta]}, \quad (3.5)$$

$$C_{\mu\nu\alpha\beta} = C_{\alpha\beta\mu\nu}. \quad (3.6)$$

$$C_{\mu\nu\alpha\beta} = C_{\mu[\nu\alpha\beta]}. \quad (3.7)$$

Moreover, when $R_{\mu\nu} = 0$, we get that $C_{\mu\nu\alpha\beta} = R_{\mu\nu\alpha\beta}$.

The Weyl tensor therefore must capture all the propagating curvature degrees of freedom, and it would be great if we could write a wave equation for it. To achieve this we first consider the Bianchi identity

$$\nabla_{\gamma}R_{\alpha\beta\mu\nu} + \nabla_{\alpha}R_{\beta\gamma\mu\nu} + \nabla_{\beta}R_{\gamma\alpha\mu\nu} = 0. \quad (3.8)$$

Taking the divergence of this identity yields

$$\square R_{\alpha\beta\mu\nu} + \nabla^\gamma \nabla_\alpha R_{\beta\gamma\mu\nu} + \nabla^\gamma \nabla_\beta R_{\gamma\alpha\mu\nu} = 0. \quad (3.9)$$

The box operator already gives this the appearance of a wave equation. We can commute the two covariant derivatives using the Ricci identity

$$\begin{aligned} \nabla_\mu \nabla_\nu R_{\alpha\beta\gamma\delta} - \nabla_\nu \nabla_\mu R_{\alpha\beta\gamma\delta} = \\ R_{\mu\nu\alpha}{}^\lambda R_{\lambda\beta\gamma\delta} + R_{\mu\nu\beta}{}^\lambda R_{\alpha\lambda\gamma\delta} + R_{\mu\nu\gamma}{}^\lambda R_{\alpha\beta\lambda\delta} + R_{\mu\nu\delta}{}^\lambda R_{\alpha\beta\gamma\lambda} \end{aligned} \quad (3.10)$$

This yields

$$\begin{aligned} \square R_{\alpha\beta\mu\nu} + 2R_{\alpha\mu}{}^\gamma{}_\lambda R_{\gamma\beta\nu\lambda} - 2R_{\alpha\nu}{}^\gamma{}_\lambda R_{\gamma\beta\mu\lambda} - 2R_{\alpha\beta}{}^\gamma{}_\lambda R_{\gamma\lambda\mu\nu} \\ - R_{\alpha}{}^\lambda R_{\lambda\beta\mu\nu} + R_{\beta}{}^\lambda R_{\lambda\alpha\mu\nu} - \nabla_\alpha \nabla^\gamma R_{\gamma\beta\mu\nu} + \nabla_\beta \nabla^\gamma R_{\gamma\alpha\mu\nu} = 0. \end{aligned} \quad (3.11)$$

Next by contracting the Bianchi identity itself we find the following identity for the divergence of the Riemann tensor

$$\nabla^\gamma R_{\gamma\nu\alpha\beta} = \nabla_\alpha R_{\beta\nu} - \nabla_\beta R_{\alpha\nu} = 2\nabla_{[\alpha} R_{\beta]\nu}. \quad (3.12)$$

Using this last identity, we can eliminate the divergences of the Riemann curvature in favour of the Ricci tensor to obtain the **Penrose wave equation**

$$\begin{aligned} \square R_{\alpha\beta\mu\nu} + 2R_{\alpha\mu}{}^\gamma{}_\lambda R_{\gamma\beta\nu\lambda} - 2R_{\alpha\nu}{}^\gamma{}_\lambda R_{\gamma\beta\mu\lambda} + 2R_{\alpha\beta}{}^\gamma{}_\lambda R_{\gamma\lambda\mu\nu} \\ - R_{\alpha}{}^\lambda R_{\lambda\beta\mu\nu} + R_{\beta}{}^\lambda R_{\lambda\alpha\mu\nu} - 2\nabla_\alpha \nabla_{[\mu} R_{\nu]\beta} + 2\nabla_\beta \nabla_{[\mu} R_{\nu]\alpha} = 0. \end{aligned} \quad (3.13)$$

This equation is build from identities that hold for any pseudo-Riemannian manifold, and therefore this equation is satisfied for the curvature tensor obtained from any metric. If in addition we impose that the metric satisfies the vacuum Einstein equation $R_{\mu\nu} = 0$, all the terms in the second line vanish. So, for vacuum solutions this turns into a wave equation for the Weyl tensor.

$$\square C_{\alpha\beta\mu\nu} + 2C_{\alpha\mu}{}^\gamma{}_\lambda C_{\gamma\beta\nu\lambda} - 2C_{\alpha\nu}{}^\gamma{}_\lambda C_{\gamma\beta\mu\lambda} + 2C_{\alpha\beta}{}^\gamma{}_\lambda C_{\gamma\lambda\mu\nu} = 0. \quad (3.14)$$

More generally, we could replace all occurrences of the Ricci tensor with the trace reversed energy-momentum tensor using the Einstein equation to find the wave equation for the curvature coupled to matter.

Let us now consider perturbations around a vacuum solution of the Einstein equation with an energy-momentum source that is order ϵ . Writting $C_{\alpha\beta\mu\nu} = \bar{C}_{\alpha\beta\mu\nu} + \epsilon \delta C_{\alpha\beta\mu\nu} + \mathcal{O}(\epsilon^2)$, the background Weyl curvature will satisfy Eq. (3.14).

To obtain the linear in ϵ part of the equation (3.13) we make the following observations

- The linear in ϵ part of the second line in Eq. (3.13) is constructed entirely from $\bar{C}_{\alpha\beta\mu\nu}$, $T_{\mu\nu}$, the background metric $\bar{g}_{\mu\nu}$, and the background covariant derivative $\bar{\nabla}_\mu$.
- The linear in ϵ part of the Riemann curvature tensor $\delta R_{\alpha\beta\mu\nu}$, consists of $\delta C_{\alpha\beta\mu\nu}$ plus terms constructed from $T_{\mu\nu}$ and the background metric $\bar{g}_{\mu\nu}$.
- We can write the action of the box operator on a generic 4-tensor $T_{\alpha\beta\mu\nu}$ as $\square T_{\alpha\beta\mu\nu} = \bar{\square} T_{\alpha\beta\mu\nu} + \epsilon B[h]_{\alpha\beta\mu\nu}{}^{\alpha'\beta'\mu'\nu'} T_{\alpha'\beta'\mu'\nu'}$ where $B[h]_{\alpha\beta\mu\nu}{}^{\alpha'\beta'\mu'\nu'}$ is formed as a linear operator on $h_{\mu\nu}$ constructed entirely from $\bar{g}_{\mu\nu}$ and $\bar{\nabla}_\mu$.
- Combining the last two observations we note that we can write the linear in ϵ part of $\square R_{\alpha\beta\mu\nu}$ as $\bar{\square} \delta C_{\alpha\beta\mu\nu} + B[h]_{\alpha\beta\mu\nu}{}^{\alpha'\beta'\mu'\nu'} \bar{C}_{\alpha'\beta'\mu'\nu'}$ plus terms depending only on $\bar{C}_{\alpha\beta\mu\nu}$, $T_{\mu\nu}$, the background metric $\bar{g}_{\mu\nu}$, and the background covariant derivative $\bar{\nabla}_\mu$.
- The linear in ϵ part of the Riemann curvature tensor $\delta R_{\alpha\beta\mu\nu}$, consists of $\delta C_{\alpha\beta\mu\nu}$ plus terms constructed from $T_{\mu\nu}$ and the background metric $\bar{g}_{\mu\nu}$.

So, if in the linear in ϵ part of the equation (3.13), we take all the terms that depend only on $T_{\mu\nu}$, the background metric $\bar{g}_{\mu\nu}$, and the background covariant derivative $\bar{\nabla}_\mu$, move them to the right hand side and collectively call them $S[T]_{\alpha\beta\mu\nu}$, we get

$$\begin{aligned} & \bar{\square} \delta C_{\alpha\beta\mu\nu} + B[h]_{\alpha\beta\mu\nu}{}^{\alpha'\beta'\mu'\nu'} \bar{C}_{\alpha'\beta'\mu'\nu'} + 2\bar{C}^\gamma{}_{\beta\nu}{}^\lambda \delta C_{\gamma\alpha\mu\lambda} + 2\bar{C}^\gamma{}_{\alpha\mu}{}^\lambda \delta C_{\gamma\beta\nu\lambda} \\ & - 2\bar{C}^\gamma{}_{\beta\mu}{}^\lambda \delta C_{\gamma\alpha\nu\lambda} - 2\bar{C}^\gamma{}_{\alpha\nu}{}^\lambda \delta C_{\gamma\beta\mu\lambda} + 2\bar{C}^\gamma{}_{\mu\nu}{}^\lambda \delta C_{\gamma\lambda\alpha\beta} + 2\bar{C}^\gamma{}_{\alpha\beta}{}^\lambda \delta C_{\gamma\lambda\mu\nu} \quad (3.15) \\ & = S[T]_{\alpha\beta\mu\nu}. \end{aligned}$$

This does not seem like much progress. While it looks like a wave equation for $\delta C_{\alpha\beta\mu\nu}$ it mixes with the equally unknown metric perturbation $h_{\mu\nu}$ in a non-trivial way. To make this useful in someway, we are going to need a miracle.

3.4 The Weyl scalars

The Weyl curvature tensor with its many components seems a highly inefficient way of capturing 10 degrees of freedom. The Newman-Penrose formalism provides a more compact way of describing these degrees of freedom. It starts by choosing a tetrad of null vectors $(l^\mu, n^\mu, m^\mu, \bar{m}^\mu)$ with properties that:

- Each vector is null, i.e. $l^\alpha l_\alpha = n^\alpha n_\alpha = m^\alpha m_\alpha = \bar{m}^\alpha \bar{m}_\alpha = 0$
- $l^\alpha n_\alpha = -1$ and $m^\alpha \bar{m}_\alpha = 1$
- All other legs are orthogonal.
- m^μ and \bar{m}^μ are complex valued and \bar{m}^μ is the complex conjugate of m^μ .

These conditions imply that

$$g_{\mu\nu} = -2l_{(\mu}n_{\nu)} + 2m_{(\mu}\bar{m}_{\nu)}.$$

This tetrad can be used to encode the 10 degrees of freedom of the Weyl curvature in 5 complex scalar fields

$$\psi_0 = C_{\alpha\beta\gamma\delta} l^\alpha m^\beta l^\gamma m^\delta, \quad (3.16a)$$

$$\psi_1 = C_{\alpha\beta\gamma\delta} l^\alpha m^\beta l^\gamma n^\delta, \quad (3.16b)$$

$$\psi_2 = C_{\alpha\beta\gamma\delta} l^\alpha m^\beta \bar{m}^\gamma n^\delta, \quad (3.16c)$$

$$\psi_3 = C_{\alpha\beta\gamma\delta} l^\alpha n^\beta \bar{m}^\gamma n^\delta, \quad (3.16d)$$

$$\psi_4 = C_{\alpha\beta\gamma\delta} n^\alpha \bar{m}^\beta n^\gamma \bar{m}^\delta, \quad (3.16e)$$

It is always possible to choose l^μ such that $\psi_0 = 0$. Such a null vector is called a **principal null vector** of the spacetime. Generically, a 4-dimensional spacetime is expected to have 4-linearly independent principal null vectors. If two principal null vectors happen to coincide then ψ_1 will vanish in addition to ψ_0 , and l^μ is called a double principal null vector.

Kerr spacetime has two double principal null vectors². If we choose both l^μ and n^μ to be a double principal null vector then we get that $\psi_0 = \psi_1 = \psi_3 = \psi_4 = 0$.

²In the Petrov classification of spacetimes this means that Kerr is type D.

A popular choice for the tetrad in Kerr that achieves this is the **Kinnersley tetrad**

$$\ell^\alpha = \left(\frac{r^2 + a^2}{\Delta}, 1, 0, \frac{a}{\Delta} \right), \quad (3.17)$$

$$n^\alpha = \left(\frac{r^2 + a^2}{2\Sigma}, -\frac{\Delta}{2\Sigma}, 0, \frac{a}{2\Sigma} \right), \quad (3.18)$$

$$m^\alpha = \frac{1}{\sqrt{2}(r + ia \cos \theta)} \left(ia \sin \theta, 0, 1, \frac{i}{\sin \theta} \right) \quad \text{and} \quad (3.19)$$

$$\bar{m}^\alpha = \frac{-1}{\sqrt{2}(r - ia \cos \theta)} \left(ia \sin \theta, 0, -1, \frac{i}{\sin \theta} \right). \quad (3.20)$$

When considering perturbed spacetimes, we need to choose a tetrad both in the background spacetime and in the perturbed spacetime. The requirement that the tetrad remains null and orthonormal fixes both tetrads up to a local Lorentz transformation. This remaining freedom introduces an additional gauge freedom.

3.5 Teukolsky Equation

A miracle happens when we try to project equation (3.15) on to a tetrad basis adapted to the double principal null vectors of Kerr spacetime. When considering the ψ_0 component, first it happens that commuting the tetrad legs with the background box operator produces terms which exactly cancel the $h_{\mu\nu}$ dependent terms in the B tensor. Second, the dependence on all other components of $\delta C_{\alpha\beta\mu\nu}$ drops out, leaving a decoupled wave equation for ψ_0 . A similar thing happens when trying to project on $(r - ia \cos \theta)^4 \psi_4$. Introducing, the notation $\Phi_2 = \psi_0$ and $\Phi_{-2} = (r - ia \cos \theta)^4 \psi_4$, using the Kinnersley tetrad the decoupled equations are given by³,

$$\begin{aligned} & - \left[\frac{(r^2 + a^2)^2}{\Delta} - a^2 \sin^2 \theta \right] \frac{\partial^2 \Phi_s}{\partial t^2} - \frac{4Mar}{\Delta} \frac{\partial^2 \Phi_s}{\partial t \partial \varphi} - \left(\frac{a^2}{\Delta} - \frac{1}{\sin^2 \theta} \right) \frac{\partial^2 \Phi_s}{\partial \varphi^2} \\ & \quad + \Delta^{-s} \frac{\partial}{\partial r} \left(\Delta^{s+1} \frac{\partial \Phi_s}{\partial r} \right) + \frac{1}{\sin \theta} \frac{\partial}{\partial \theta} \left(\sin \theta \frac{\partial \Phi_s}{\partial \theta} \right) \\ & + 2s \left[\frac{a(r - M)}{\Delta} + \frac{i \cos \theta}{\sin^2 \theta} \right] \frac{\partial \Phi_s}{\partial \varphi} + 2s \left[\frac{M(r^2 - a^2)}{\Delta} - r - ia \cos \theta \right] \frac{\partial \Phi_s}{\partial t} \\ & \quad - (s^2 \cot^2 \theta - s) \Phi_s = S_s [T_{\mu\nu}], \end{aligned} \quad (3.21)$$

³For the gory details of how to get here see [3].

where $S_s[T_{\mu\nu}]$ is a second order differential operator that produces the projected source term for $T_{\mu\nu}$. This is the **Teukolsky equation**. (It turns out that this same equation with $s = \pm 1$ describes solutions to the Maxwell equations on a curved background. With $s = 0$ it describes a massless scalar field, and with $s = 1/2$ a massless Dirac field.)

The perturbed Weyl scalars ψ_0 and ψ_4 have some useful properties in Kerr spacetimes.

First of all they are gauge invariant. Since they are scalar quantities whose background values are zero they are insensitive to normal gauge transformations. Moreover, infinitesimal rotations of the tetrad only mix the background values of ψ_0 and ψ_1 into the perturbed value of ψ_0 (or ψ_4 and ψ_3 into ψ_4). Since both background values vanish, infinitesimal rotations of the tetrad cannot change ψ_0 (or ψ_4).

Second, it turns out that ψ_0 (or ψ_4) contain almost all there is to know about metric perturbation in Kerr spacetime, as expressed by the following theorem.

Theorem (Wald [4]). *Suppose $h_{\mu\nu}$ and $h'_{\mu\nu}$ are (suitably well-behaved) solutions to the Einstein equation, such that the perturbation to the Weyl scalar ψ_0 (or ψ_4) is the same for both perturbations. Then*

$$h_{\mu\nu} - h'_{\mu\nu} = \nabla_{(\mu} \xi_{\nu)} + c_M \frac{\partial g^{\text{Kerr}}}{\partial M} + c_a \frac{\partial g^{\text{Kerr}}}{\partial a},$$

for some gauge vector ξ_μ and constants c_M and c_a .

So, ψ_0 “knows” everything about the vacuum metric perturbation except the gauge (since it is itself gauge invariant) and perturbation of the mass and spin of the Kerr background (since $\psi_0 = 0$ on any Kerr background.) Furthermore, we get,

Corollary.

$$\psi_0[h] = \psi_0[h'] \Leftrightarrow \psi_4[h] = \psi_4[h'].$$

3.5.1 Separation of Variables

Note that the left-hand side of the Teukolsky equation does not contain any explicit dependence on t and ϕ . We can thus do a Fourier transform with respect to t and ϕ to get

$$\Phi_s(t, r, \theta, \phi) = \int d\omega \sum_m \hat{\Phi}_{sm\omega}(r, \theta) e^{i(m\phi - \omega t)}, \quad (3.22)$$

and

$$\begin{aligned}
& \Delta^{-s} \frac{\partial}{\partial r} \left(\Delta^{s+1} \frac{\partial \hat{\Phi}_{sm\omega}}{\partial r} \right) \\
& + \left(\frac{(\omega(r^2 + a^2) - am - is(r - M))^2 + s^2(r - M)^2}{\Delta} + 2am\omega + 4is\omega r \right) \hat{\Phi}_{sm\omega} \\
& + \frac{1}{\sin \theta} \frac{\partial}{\partial \theta} \left(\sin \theta \frac{\partial \hat{\Phi}_{sm\omega}}{\partial \theta} \right) - \left(\frac{(m + s \cos \theta)^2}{\sin^2 \theta} + a^2 \omega^2 \sin^2 \theta + 2sa\omega \cos \theta - s \right) \hat{\Phi}_{sm\omega} \\
& = \hat{S}_{sm\omega}[T_{\mu\nu}].
\end{aligned} \tag{3.23}$$

The left-hand side of the equation separates into part with only explicit dependence on r and a second part that depends on θ .

The polar operator appearing on the left-hand side,

$$\frac{1}{\sin \theta} \frac{\partial}{\partial \theta} \left(\sin \theta \frac{\partial}{\partial \theta} \right) - \frac{(m + s \cos \theta)^2}{\sin^2 \theta} - a^2 \omega^2 \sin^2 \theta - 2sa\omega \cos \theta + s, \tag{3.24}$$

is a Sturm-Liouville operator. Consequently, it has a real eigenvalues $(-\lambda_{slm\omega} - 2ma\omega)$ with $l \geq l_0 \max(|s|, |m|)$ such that $0 \leq \lambda_{sl_0 m\omega} < \lambda_{s(l_0+1)m\omega} < \dots$, and corresponding real-valued eigenfunctions $S_{slm\omega}(\theta)$ that satisfy

$$\int_{-1}^1 S_{slm\omega}(\theta) S_{sl'm\omega}(\theta) d\cos \theta = \delta_{ll'},$$

and span the space of continuous functions of the interval $[0, \pi]$.

This functions are known as **spin-weighted spheroidal harmonics** with spin-weight s and spheroidicity $a\omega$. In the limit $a\omega \rightarrow 0$, these reduce to $\lambda_{slm\omega} = l(l+1) - s(s+1)$, and the more familiar spin-weighted spherical harmonics $Y_{slm}(\theta, \phi)$ (when paired with the $e^{im\phi}$ from the Fourier expansion.

We can therefore further expand $\hat{\Phi}_{sm\omega}(r, \theta)$ and source $\hat{S}_{sm\omega}[T_{\mu\nu}]$ in the basis of spin-weighted spheroidal harmonics

$$\hat{\Phi}_{sm\omega}(r, \theta) = \sum_{l \geq |s|} R_{slm\omega}(r) S_{slm\omega}(\theta), \tag{3.25}$$

and

$$\hat{S}_{sm\omega}[T_{\mu\nu}](r, \theta) = \sum_{l \geq |s|} \hat{S}_{slm\omega}[T_{\mu\nu}](r) S_{slm\omega}(\theta). \tag{3.26}$$

Plugging this into (3.23), we find that the radial coefficients satisfy

$$\Delta^{-s} \frac{\partial}{\partial r} \left(\Delta^{s+1} \frac{\partial R_{slm\omega}}{\partial r} \right) - V_{slm\omega} R_{slm\omega} = \hat{S}_{slm\omega}[T_{\mu\nu}], \tag{3.27}$$

with

$$V_{slm\omega} = -\frac{(\omega(r^2 + a^2) - am - is(r - M))^2 + s^2(r - M)^2}{\Delta} - 4is\omega r + \lambda_{slm\omega}. \quad (3.28)$$

This is the **radial Teukolsky equation**.

3.5.2 Homogeneous solutions, Asymptotic Behaviour, and Boundary conditions

$$\Delta^{-s} \frac{\partial}{\partial r} \left(\Delta^{s+1} \frac{\partial R_{slm\omega}}{\partial r} \right) - V_{slm\omega} R_{slm\omega} = 0, \quad (3.29)$$

To study the asymptotic behaviour of homogeneous (i.e. $\hat{S}_{slm\omega} = 0$) solutions to the radial Teukolsky equation near the horizon and near infinity, it is useful to make the follow transformation

$$\tilde{R} = \Delta^{s/2} \sqrt{r^2 + a^2} R \quad (3.30)$$

$$\frac{dr^*}{dr} = \frac{r^2 + a^2}{\Delta}, \quad (3.31)$$

$$r^* = r + \frac{Mr_+}{\sqrt{M^2 - a^2}} \log \frac{r - r_+}{2M} - \frac{Mr_-}{\sqrt{M^2 - a^2}} \log \frac{r - r_-}{2M}, \quad (3.32)$$

where r^* is the Kerr tortoise coordinate. This turns the homogeneous radial equation into (suppressing the subscripts $slm\omega$ for brevity).

$$\frac{d^2 \tilde{R}}{dr^{*2}} + U \tilde{R} = 0, \quad (3.33)$$

with

$$U = \frac{(\omega(r^2 + a^2) - am - is(r - M))^2 + s^2(r - M)^2 + \Delta(4is\omega r - \lambda)}{(r^2 + a^2)^2} - G^2 - \frac{dG}{dr^*}, \quad (3.34)$$

and

$$G = \frac{s(r - M)}{r^2 + a^2} + \frac{r\Delta}{(r^2 + a^2)^2}. \quad (3.35)$$

For large r (and thus $r^* \rightarrow \infty$), we get that

$$U = \omega^2 + \frac{2is\omega}{r} + \mathcal{O}(r^{-2}) \quad (3.36)$$

Consequently, we get the asymptotic solutions near infinity

$$\tilde{R} \underset{r \rightarrow \infty}{\propto} \frac{1}{r^{\pm s}} \exp(\pm i\omega r^*) \quad (3.37)$$

our translating back to our original radial field R

$$R \underset{r \rightarrow \infty}{\propto} \frac{1}{r^{2s+1}} \exp(i\omega r^*) \quad \text{or} \quad R \underset{r \rightarrow \infty}{\propto} \frac{1}{r} \exp(-i\omega r^*). \quad (3.38)$$

Near the horizon as $r \rightarrow r_+$ (and $r^* \rightarrow -\infty$), we get

$$U = \left(k - is \frac{\sqrt{M^2 - a^2}}{2Mr_+} \right)^2 + \mathcal{O} \Delta, \quad (3.39)$$

where

$$k = \omega - m\Omega_+ \quad (3.40)$$

is the frequency of the mode shifted by the rotation frequency of the outer horizon $\Omega_+ = \frac{a}{2Mr_+}$. Consequently, the asymptotic behaviour of the solutions near the horizon is

$$\tilde{R} \underset{r \rightarrow r_+}{\propto} \exp \left(\pm i \left(k - is \frac{\sqrt{M^2 - a^2}}{2Mr_+} \right) r^* \right) \quad (3.41)$$

$$= \exp \left(\pm is \frac{\sqrt{M^2 - a^2}}{2Mr_+} r^* \right) \exp(\pm ikr^*) \quad (3.42)$$

$$\approx \Delta^{\pm s/2} \exp(\pm ikr^*), \quad (3.43)$$

where we used that near the horizon

$$r^* \approx \frac{Mr_+}{\sqrt{M^2 - a^2}} \log \frac{r - r_+}{2M} \approx \frac{Mr_+}{\sqrt{M^2 - a^2}} \log \Delta. \quad (3.44)$$

For our original field R this translates to

$$R \underset{r \rightarrow r_+}{\propto} \exp(ikr^*) \quad \text{or} \quad R \underset{r \rightarrow r_+}{\propto} \Delta^{-s} \exp(-ikr^*). \quad (3.45)$$

So, we find that a general solution of the homogeneous radial Teukolsky equation $R_{slm\omega}$ has the following asymptotic behaviour (for $\omega \neq 0$)

$$R_{slm\omega} = \begin{cases} \frac{A_{slm\omega}^{\mathcal{I}^+}}{r^{2s+1}} \exp(i\omega r^*) + \frac{A_{slm\omega}^{\mathcal{I}^-}}{r} \exp(-i\omega r^*) & \text{as } r \rightarrow \infty \\ A_{slm\omega}^{\mathcal{H}^-} \exp(ikr^*) + A_{slm\omega}^{\mathcal{H}^+} \Delta^{-s} \exp(-ikr^*) & \text{as } r \rightarrow r_+ \end{cases} \quad (3.46)$$

The A coefficients have the following interpretations:

- $A_{slm\omega}^{\mathcal{I}^+}$ is (related to) the amplitude of GWs in the solution $R_{slm\omega}$ traveling **out** to future null infinity \mathcal{I}^+ .

- $A_{slm\omega}^{\mathcal{I}^-}$ is (related to) the amplitude of GWs in the solution $R_{slm\omega}$ coming **in** from past null infinity \mathcal{I}^- .
- $A_{slm\omega}^{\mathcal{H}^+}$ is (related to) the amplitude of GWs in the solution $R_{slm\omega}$ falling **down** the future event horizon \mathcal{H}^+ .
- $A_{slm\omega}^{\mathcal{H}^-}$ is (related to) the amplitude of GWs in the solution $R_{slm\omega}$ coming **up** from the past event horizon \mathcal{H}^- .

The homogeneous radial Teukolsky equation is a second-order ordinary differential equation. Hence it has a two dimensional space of solutions. We can use our knowledge about the asymptotic behaviour of a general solution at infinity and the horizon to impose boundary conditions to identify the elements of a basis for this solution space. The most popular choice involves putting boundary conditions on past null infinity \mathcal{I}^- and the past horizon \mathcal{H}^- . The two basis elements in this basis are:

- The **ingoing** solution $R_{slm\omega}^{\text{in}}$ is the homogeneous solution that only has waves coming in from past null infinity \mathcal{I}^- , but no waves coming up from the past horizon \mathcal{H}^- . It is defined by setting $A_{slm\omega}^{\mathcal{H}^-} = 0$ and normalized by $A_{slm\omega}^{\mathcal{H}^+} = 1$.
- The **upgoing** solution $R_{slm\omega}^{\text{up}}$ is the homogeneous solution that has waves coming up from the past event horizon \mathcal{H}^- , but no waves coming in from past null infinity \mathcal{I}^- . It is defined by setting $A_{slm\omega}^{\mathcal{I}^-} = 0$ and normalized by $A_{slm\omega}^{\mathcal{H}^+} = 1$.

Together these two span the solutions for the homogeneous radial Teukolsky equation for any real non-zero frequency ω .

In addition people sometimes use the “time-reverse” solutions for their basis:

- The **outgoing** solution $R_{slm\omega}^{\text{out}}$ defined by setting $A_{slm\omega}^{\mathcal{H}^+} = 0$ and normalized by $A_{slm\omega}^{\mathcal{H}^-} = 1$.
- The **downgoing** solution $R_{slm\omega}^{\text{down}}$ defined by setting $A_{slm\omega}^{\mathcal{I}^+} = 0$ and normalized by $A_{slm\omega}^{\mathcal{H}^-} = 1$.

Generically, any pair of $(R_{slm\omega}^{\text{in}}, R_{slm\omega}^{\text{out}}, R_{slm\omega}^{\text{up}}, R_{slm\omega}^{\text{down}})$ can be used as a basis, and the other two can be written in terms of them, e.g.

$$R_{slm\omega}^{\text{down}} \propto R_{slm\omega}^{\text{in}} - R_{slm\omega}^{\text{up}}, \quad \text{and} \quad (3.47)$$

$$R_{slm\omega}^{\text{up}} \propto R_{slm\omega}^{\text{out}} - R_{slm\omega}^{\text{down}}. \quad (3.48)$$

3.5.3 Particular solutions

$$\Delta^{-s} \frac{\partial}{\partial r} \left(\Delta^{s+1} \frac{\partial R_{slm\omega}}{\partial r} \right) - V_{slm\omega} R_{slm\omega} = \hat{S}_{slm\omega}[T_{\mu\nu}], \quad (3.49)$$

To find particular solutions to the inhomogeneous Teukolsky equation we can follow a Green's function approach. If we first solve

$$\Delta^{-s} \frac{\partial}{\partial r} \left(\Delta^{s+1} \frac{\partial G_{slm\omega}(r, r_0)}{\partial r} \right) - V_{slm\omega} G_{slm\omega}(r, r_0) = \delta(r - r_0), \quad (3.50)$$

the particular solution for a general source is then given by

$$R_{slm\omega} = \int_{r_+}^{\infty} G(r, r_0) \hat{S}_{slm\omega}[T_{\mu\nu}] dr_0. \quad (3.51)$$

To solve for the Green's function we first need to choose boundary conditions. Usually the physically relevant choices are the “retarded” boundary conditions, where for large r , the Green's function $G(r, r_0)$ satisfies outgoing boundary conditions (i.e. no waves from \mathcal{I}^-), and incoming boundary conditions (no waves from \mathcal{H}^-) near the horizon. With these choices the Green's function is given by

$$G_{slm\omega}(r, r_0) = \begin{cases} \frac{R_{slm\omega}^{\text{up}}(r_0) R_{slm\omega}^{\text{in}}(r)}{W[R_{slm\omega}^{\text{in}}, R_{slm\omega}^{\text{up}}](r_0)} & r < r_0 \\ \frac{R_{slm\omega}^{\text{in}}(r_0) R_{slm\omega}^{\text{up}}(r)}{W[R_{slm\omega}^{\text{in}}, R_{slm\omega}^{\text{up}}](r_0)} & r > r_0, \end{cases} \quad (3.52)$$

where $W[R_{slm\omega}^{\text{in}}, R_{slm\omega}^{\text{up}}](r_0)$ is the Wronskian

$$W[R_{slm\omega}^{\text{in}}, R_{slm\omega}^{\text{up}}](r) = R_{slm\omega}^{\text{in}} \frac{dR_{slm\omega}^{\text{up}}}{dr} - \frac{dR_{slm\omega}^{\text{in}}}{dr} R_{slm\omega}^{\text{up}}. \quad (3.53)$$

3.6 Quasinormal Modes

In the last section, we discussed using $R_{slm\omega}^{\text{in}}$ and $R_{slm\omega}^{\text{up}}$ as a basis for all vacuum, and how they can be used to construct general particular solutions. However, what happens when $R_{slm\omega}^{\text{in}} = R_{slm\omega}^{\text{up}}$? Can there be vacuum solutions that simultaneously satisfy outgoing and ingoing boundary conditions, i.e. where there are no incoming waves from either past null infinity or the past horizon? For generic ω the answer is no, but for special values of ω the answer is yes. These frequencies are known as the **quasinormal modes** (or **QNMs**) of a black hole. These QNMs act like a “finger print” of the black hole.

We start by citing an important result regarding a Kerr black hole's QNMs

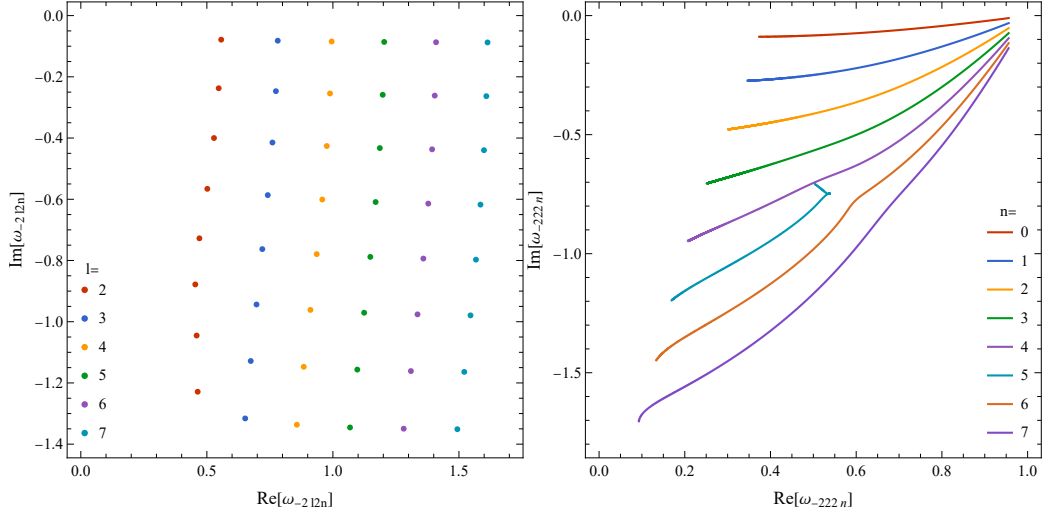


Figure 3.1: On the left the QNMs for a Kerr black hole with spin $a = 0.75M$ and $m = 2$. On the right the QNMs with $l = m = 2$ for Kerr black holes with spin between $a = 0$ and $a = 0.999M$. (Data from <https://pages.jh.edu/eberti2/ringdown/>.)

Theorem (Kerr mode stability). *All quasinormal modes of a Kerr black hole have $\text{im } \omega < 0$.*

This theorem guarantees that the time dependence of any Kerr QNM ($\exp(-i\omega t)$) is decaying in nature, and there are no vacuum modes that grow out of control.

This also means that for each l and m there will be a QNM with the largest imaginary frequency. This will be the longest lived mode with those l and m , and is called the **fundamental** mode. The QNMs with a certain l and m are numbered by natural numbers n in order of descending imaginary part (i.e. $n = 0$ is the fundamental mode.) The modes with $n > 0$ are referred to as **overtones** (despite generally having a lower real part of the frequency.)

Lemma 5. *If ω_{lmn} is a quasinormal mode, then so is $-\omega_{l(-m)n}^*$.*

The intuitive picture of quasinormal modes is that they consist of waves travelling along the lightring of the Kerr black hole, decaying because of the unstable nature of this orbit. For small enough wave packets, i.e. large l , we indeed see that $\text{re } \omega \approx l\Omega_{LR}$ and $\text{im } \omega$ roughly corresponds to the Lyapunov exponent characterizing how unstable it is.

The QNM frequencies are determined by the parameters of the background black hole (i.e. the mass M and the spin a). The spectrum of QNMs

thus forms a unique “fingerprint” for the black hole.

If we perturb a black hole (e.g. by dropping something into it) it will settle down exponentially to a member of the Kerr family, with the final stage being a linear combination of the quasi-normal modes. This process is called **ringdown**.

Bibliography

- [1] Black Hole Perturbation Toolkit. (bhptoolkit.org).
- [2] Robert H. Boyer and Richard W. Lindquist. Maximal analytic extension of the Kerr metric. **J. Math. Phys.**, 8:265, 1967.
- [3] Michael P. Ryan. Teukolsky equation and Penrose wave equation. **Phys. Rev. D**, 10:1736–1740, 1974.
- [4] Robert M. Wald. On perturbations of a Kerr black hole. **J. Math. Phys.**, 14(10):1453–1461, 1973.